Article

Elucidating the Relations between Gut Bacterial Composition and the Plasma and Fecal Metabolomes of Antibiotic Treated Wistar Rats

Aishwarya Murali [1]**, Varun Giri** [1]**, Hunter James Cameron** [2]**, Christina Behr** [1]**, Saskia Sperber** [1]**, Hennicke Kamp** [1]**, Tilmann Walk** [3] **and Bennard van Ravenzwaay** [1,*]

[1] BASF SE, 67056 Ludwigshafen, Germany; aishwarya.murali@basf.com (A.M.); varun.giri@basf.com (V.G.); NinaBehr1@gmx.de (C.B.); saskia.sperber@basf.com (S.S.); hennicke.kamp@basf.com (H.K.)
[2] BASF Plant Science LP, Research Triangle Park, Raleigh, NC 27709, USA; hunter.james.cameron@basf.com
[3] BASF Metabolome Solutions GmbH, 10589 Berlin, Germany; tilmann.walk@basf.com
[*] Correspondence: bennard.ravenzwaay@basf.com; Tel.: +49-621-60-56419

Abstract: The gut microbiome is vital to the health and development of an organism, specifically in determining the host response to a chemical (drug) administration. To understand this, we investigated the effects of six antibiotic (AB) treatments (Streptomycin sulfate, Roxithromycin, Sparfloxacin, Vancomycin, Clindamycin and Lincomycin hydrochloride) and diet restriction (–20%) on the gut microbiota in 28-day oral toxicity studies on Wistar rats. The fecal microbiota was determined using 16S rDNA marker gene sequencing. AB-class specific alterations were observed in the bacterial composition, whereas restriction in diet caused no observable difference. These changes associated well with the changes in the LC–MS/MS- and GC–MS-based metabolome profiles, particularly of feces and to a lesser extent of plasma. Particularly strong and AB-specific metabolic alterations were observed for bile acids in both plasma and feces matrices. Although AB-group-specific plasma metabolome changes were observed, weaker associations between fecal and plasma metabolome suggest a profound barrier between them. Numerous correlations between the bacterial families and the fecal metabolites were established, providing a holistic overview of the gut microbial functionality. Strong correlations were observed between microbiota and bile acids, lipids and fatty acids, amino acids and related metabolites. These microbiome–metabolome correlations promote understanding of the functionality of the microbiome for its host.

Keywords: gut microbiome; metabolomics; antibiotics; repeated oral toxicity study; 16S gene sequencing; DADA2; correlation analysis; metabolic capacity

1. Introduction

The gut microbiome plays an essential role in host health and well-being by maintaining physiological homeostasis [1]. The human gastrointestinal tract has been known to possess more than 10^{14} microbial cells and hence over 100 times more genes than the human genome [2]. Bacterial cells are present in the human gut by 2–3 orders of magnitude more compared to the eukaryotes and archaea [3]. The gut flora is easily altered by several factors including host health, medication, environment, diet, age, host genetics, and immune system [4,5]. Specifically, host diet and antibiotic usage have important influences in altering the composition of the gut microbiome [6].

Bacteria carry out microbiome-associated reactions that have been well characterized including tyrosine and tryptophan metabolism, glycerol and mucin production, hydroxylation, glucuronidation and short-chain fatty acid (SCFA) metabolism [6,7]. Zimmermann et al., 2019 provided an outline of the drug-metabolizing activity of human gut bacteria and discovered that about 2/3 of the drugs are metabolized by at least one bacterial strain [4]. Maier et al., 2018 elucidated gut microbial compositional dysbiosis influenced by non-antibiotic drugs [8]. Findings like these promote a better understanding of microbiome

metabolism and metabolism-related microbiome–host interactions [6]. The gut bacteria work hand in hand with the host immune system development that in turn influences signaling pathways of multiple organs such as gastrointestinal tract (GI), liver, muscle, and brain. In addition to the production of metabolites that are advantageous for the host health and phenotype, gut bacteria also contribute to disease risks such as obesity, diabetes, colitis, neurodegenerative disorders and several other long-term health effects [9–12]. As species-specific gut microbiome contributions are highly likely, this research will help in identifying the modes of actions and human relevance.

Therefore, the understanding of microbial biotransformation is essential for the field of toxicology. While toxicity studies predominantly consider the role of the liver [13] for metabolism, gut-mediated microbiome metabolism is poorly characterized. The aim of this study was to investigate how families and species of the intestinal microbiome contribute to the status of natural components, referred to as metabolites, which are subsequently available for absorption from the intestinal tract. To investigate this, we determined microbiome communities as well as fecal and plasma metabolites. We introduced changes in the microbiome by the administration of several antibiotics and correlated the induced community changes with the changes in the fecal metabolome. Subsequently, the fecal metabolome changes were compared with the plasma metabolome. The correlation analysis now provides a connectivity map and shows how individual microbiome communities are responsible for the formation of fecal metabolites and how these are connected with the plasma metabolome.

Antibiotics are known to induce a gut compositional dysbiosis, making it possible to compare rat fecal and plasma metabolomes [14–17]. Targeted metabolite measurements of classes such as carbohydrates, amino acids, nucleic acids or fatty acids and their derivatives were used to identify specific metabolite patterns associated with the administration of different antibiotics [18].

We have used a standardized procedure to determine the metabolome of test substance since 2004. Metabolome data are uploaded in the MetaMap®Tox database to compare a given substance with the other metabolome profiles available in the database. The MetaMap®Tox or MMTox database comprises data for about 1000 compounds whose modes of action have been determined and is also used for statistical and visualization tools as described in van Ravenzwaay et al., 2016 [19]. It not only gives us the ability to determine the statistical significance of regulated metabolites but also allows the assessment of whether a specific metabolite value has ever been observed in control animals, providing a historical range of what is normal.

To expand the findings from the previous work of Behr et al. [14–16], we investigated the inter-omic correlations between the gut community and the fecal and plasma metabolomes. The standardized study protocol for the correlation analysis is shown in Figure 1. Gut microbial composition of Wistar rats was assessed by 16S rDNA gene sequencing of fecal samples. Subsequently, the fecal metabolome was analyzed and correlated with the microbiome community changes. Finally, we determine the plasma metabolomes of the antibiotic-treated rats to establish a correlation between the gut microbial changes and both metabolome profiles. As treatment with compounds such as antibiotics frequently results in a reduction of food consumption at higher dose levels, we include in our studies a group of rats in which only the food supply was reduced to take into account possible effects of reduced food consumption.
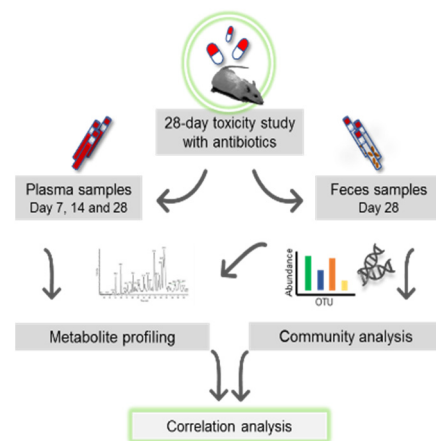
Figure 1. The schematic diagram shows the overall process of a 28-day oral toxicity study with plasma and feces sampling. Plasma sampling was conducted on days 7, 14, and 28 of the study and feces was sampled on the day of necropsy, day 28. Subsequently, plasma and feces samples were subjected to metabolomics and feces to 16S community analysis. With both omic datasets, correlation analyses were carried out.

2. Materials and Methods

2.1. Ethical Statement

The studies were approved by the BASF Animal Welfare Body, with the permission of the local authority, the Landesuntersuchungsamt Rheinland-Pfalz (approval number 23 177-07/G 13-3-016, approved on 10 February 2016). The studies were performed in an AAALAC-approved (Association for Assessment and Accreditation of Laboratory Animal Care International) laboratory in accordance with the German Animal Welfare Act and the effective European Council Directive.

2.2. Animals and Maintenance Conditions

Briefly, male and female Wistar rats (CrI:WI(Han)) were supplied by Charles River, Germany, and were 70 ± 1 days old at the beginning of the studies. The animals were single- and group-caged in the four studies reported in this publication. For the grouped caging conditions, the animals (5 rats per sex and cage in one group) were maintained in an air-conditioned room at a temperature of 20 to 24 °C, a relative humidity of 30 to 70%, and a 12 h light/12 h dark cycle. Ground Kliba mouse/rat maintenance diet "GLP" was supplied by Provimi Kliba SA, Kaiseraugst, Switzerland. Diet and drinking water were available ad libitum (except 16–20 h before sampling) and regularly assayed for chemical contaminants and the presence of microorganisms.

2.3. Study Design

Four independent 28-day oral toxicity studies in Wistar rats were performed following the principles of the OECD 407 test guideline. Animal handling, treatment, and clinical examinations have been described earlier [14,15,17]. All the animals were checked daily for any clinically abnormal signs and mortalities. Food consumption was determined on study days 6, 13 and 27. Additionally, body weights of all the animals were determined before the start of the administration period in order to randomize the animals and also on study days 6, 13 and 27. At the end of the treatment periods, the animals were sacrificed by decapitation under isoflurane anesthesia. These studies involved treatments with antibiotics belonging to five different classes (see Table 1). Furthermore, one group of animals was provided with a reduced amount of diet (approx. 20% less compared to ad libitum food intake) to observe their influence on gut dysbiosis and gut metabolic functions. Metabolite profiling was conducted on plasma, cecum and fecal samples, and microbiome profiling was conducted on the fecal samples.

Table 1. Compounds used, dose levels, caging type and class of antibiotics. All compounds were administered orally by gavage.

Study Number	Treatment	Low Dose (mg/kg bw/day)	High Dose (mg/kg bw/day)	Caging	Form of Preparation	Class of Antibiotics
1–4	Control diet	-	-	Grouped (5)	-	-
1	Vancomycin	50	400	Grouped (5)	in ultra-pure water	Glycopeptides
1	Streptomycin sulfate	100	450	Grouped (5)	in water containing 0.5% CMC [a]	Aminoglycosides
1	Roxithromycin	200	600	Grouped (5)	in water containing 0.5% CMC [a]	Macrolides
2	Sparfloxacin	200	600	Grouped (5)	in water containing 0.5% CMC [a]	Fluoroquinolones
3	Restricted diet (−20%)	-	-	Single (1)	-	-
4	Clindamycin hydrochloride	200	600	Grouped (5)	in ultra-pure water	Lincosamides
4	Lincomycin hydrochloride	300	10000	Grouped (5)	in water containing 0.5% CMC [a]	Lincosamides

[a] carboxymethyl cellulose: Tylose CB30000; Single caging = one rat per cage; kg bw = kilogram body weight.

2.4. Treatment of Animals with Antibiotics

Treatment groups involved 5 rats per sex and dose group. Dose levels of the antibiotics were selected such that the low dose (LD) and high dose (HD) would induce low yet reversible toxicity of the antibiotics. The antibiotics were gavaged daily using an appropriate vehicle for animals. The substances were administered in four separate studies (study 1: Vancomycin, Streptomycin, Roxithromycin; study 2: Sparfloxacin, Lincomycin; study 3: single caged restricted diet (−20%) fed study; study 4: Clindamycin study), each with a concurrent control group of 10 animals per sex, to allow for comparisons. Dose-levels, grouping of animals and form of preparation of the antibiotics are summarized in Table 1.

2.5. Sampling of Plasma, Cecum and Feces for Omics Profiling

Between 7:30 and 10:30 h, on study days 7, 14 and 28 blood samples were taken from the retro-bulbous sinus of all the rats under isoflurane anesthesia (1.0 mL K-EDTA blood) after overnight fasting. The blood samples were centrifuged (10 °C, 20,000× g, 2 min), and the EDTA plasma was separated. The EDTA plasma samples were snap-frozen with liquid nitrogen gas to keep the samples devoid of oxygen and stored at −80 °C until metabolome profiling was performed. Cecum and feces samples were sampled during necropsy on day 28. Fecal samples were carefully removed from the rectum at the end of the study after the last administration of the test substances. The samples were collected in pre-cooled (dry-ice) vials, immediately snap-frozen in liquid nitrogen and stored at −80 °C until further profiling was performed. The blood plasma, cecum and fecal samples were used for metabolome analysis as standardized in Behr et al. 2017 [16]. The feces samples were additionally used for 16S bacterial profiling.

2.6. DNA Isolation and Bacterial 16S rDNA Gene Amplicon Sequencing

DNA was isolated from the fecal samples using InnuPREP stool DNA Kit (Analytik Jena GmbH, Jena, Thuringia, Germany) according to the manufacturer's instructions as published in Behr et al. 2018 [15]. Based on observations made during the process, the incubation temperature for the cells' lysis was lowered to 75 °C. DNA yield and

integrity were assessed using a Nanodrop. Samples were sent to IMGM® laboratories (Martinsried, Germany) for PCR, library preparation and sequencing. DNA was amplified using 16S V3-V4 primers (Bakt_341F: 5′-CCTACGGGNGGCWGCAG-3′ and Bakt_805r: 5′-GACTACHVGGGTATCTAATCC-3′). Sequencing was performed on the Illumina MiSeq® next-generation sequencing system (Illumina Inc., San Diego, CA, USA). Signals were processed to fastq files, and the resulting 2 × 250 bp reads were demultiplexed using the MiSeq®-inherited MiSeq Control Software (MCS) v2.5.0.5.

2.7. Metabolome Profiling of Plasma, Cecum and Fecal Matrices

Blood plasma, cecum and fecal samples were used for mass-spectrometry based measurements of metabolites using GC-MS (gas chromatography-mass spectrometry) and LC–MS/MS [20]. First, removal of proteins from 60 μL of plasma samples was performed using 200 μL acetonitrile via precipitation reaction. The polar and non-polar fractions using water and a mixture of ethanol and dichloromethane (1:2, *v/v*)). Five milligrams of feces was subjected to freeze-drying and grinding prior to extraction and extracted with a mixture of acetonitrile, water, ethanol and dichloromethane in a sample tube containing a 3 mm stainless steel ball using a Bead Ruptor (Omni International Inc., Kennesaw, GA, USA). Additionally, dichloromethane was used for phase separation. Non-polar fraction was treated with methanol at acidic pH to form fatty acid methyl esters from free fatty acids as well as hydrolyzed complex lipids. Further, oxo-groups of the polar and non-polar fractions were converted to O-methyl-oximes with O-methyl-hydroxylamine hydrochloride and pyridine, followed by the addition of a silylating agent before analysis [15,17,21].

Both the fractions were re-prepared in appropriate solvent mixtures for LC–MS/MS analysis. LC analyses were performed by gradient elution on reverse-phase separation columns and mass spectrometric detection was conducted with targeted and highly sensitive MRM (Multiple Reaction Monitoring) profiling in parallel to a full-screen analysis as described in patent WO2003073464 [21]. The acquisition in scan mode m/z ratio 15–600 for polar compounds and m/z ratio 40–600 for lipid compounds were applied for GC-MS analysis. MRM profiles for all the detected analytes were determined using standard solutions. The conditions applied for GC– and LC–MS are described as follows:

GC–MS conditions: CTC GC PAL, Agilent 6890 GC gas chromatograph, 5973 MSD mass spectrometer, gradient: 70–340 °C, carrier gas: helium, acquisition in scan mode m/z 15–600 (polar compounds)/m/z 40–600 (lipid compounds) [15,17,21].

LC–MS conditions: Agilent 1100 HPLC System, AB Sciex API 4000 mass spectrometer, gradient elution for polar compounds with water/acetonitril/ammonium formate, gradient elution for lipid compounds with water/methanol/methyl tert-butyl ether/formic acid, MRM and Q3 Scan m/z 100–1000 [15,17,21].

Data for GC-MS and LC–MS/MS were normalized to the medians of reference samples that were obtained from pooled aliquots of all the samples in order to account for inter- and intra-instrumental biases. About 274 semi-quantitative metabolites were measured using the single peak signals in plasma samples according to methods optimized in patent WO2007012643A1 [15,17,21], which resulted in ratios/values that represented a relative change in the metabolites w.r.t control data. About 248 of these 274 detected metabolites were chemically identified, and 26 remain structurally unidentified. A total of 208 semi-quantitative metabolites were measured from feces samples, out of which 177 were chemically identified and 31 were structurally unidentified.

2.8. Targeted Bile Acid Profiling of Plasma and Fecal Matrices

Blood plasma and feces samples from the low-dose groups of controls and antibiotic-treated animals that were stored in −80 °C were used for bile acid profiling. Measurements of bile acids were performed using UHPLC–ESI-MS/MS consisting of a Waters Acquity UHPLC system coupled with an SCIEX 5500 Triple Quad™ LC–MS/MS system equipped with an ESI ion source. This facilitated successful measurements of 20 different bile acids. To enhance accuracy and precision of the data, the method provided seven calibration

standards including a mixture of three isotope-labeled internal standards along with a quality control sample. Firstly, 5 mg of dried feces samples were extracted with 1 mL extraction solvent (ethanol (95%)/NaOH [0.1 N]) with an incubation of 30 min in an ultrasonic bath followed by a 10 min centrifugation step at 14,000 rpm, 4 °C [16,21]. The supernatant from the samples was removed and used for further analysis. Further, 10 μL of extracted feces/plasma samples were resuspended with 10 μL of internal standards mixture and added onto filter spots suspended in the wells of a 96-well filter plate (PALL Corporation, Port Washington, NY, USA, AcroPrep^TM PTFE 0.2 μm) fixed on top of a deep-well plate followed by extraction with 100 μL methanol by shaking at 600 rpm for 20 min on an Eppendorf ThermoMixer C (Eppendorf AG, Hamburg, Germany) as stated in Behr et al. 2020. The elution step after extracting using methanol was performed by centrifugation at 5700 rpm for 5 min onto the deep-well plate, which was then detached from the 96-well filter plate. Sixty microliters of Milli-Q® water was added to the eluates by shaking briefly at 600 rpm for 5 min, after which the samples on the plate were analyzed by LC–MS/MS [16,21].

All the targeted isobaric bile acids were baseline-separated using ultrahigh-pressure liquid chromatography (UPLC) as described previously in Behr et al. 2020. UPLC systems were briefly used at a flow rate of 0.5–1 mL/min. Water with 0.01% formic acid and 10 mM ammonium acetate was mobile phase A, whereas mobile phase B was 30% (*v/v*) acetonitrile/methanol with 0.01% formic acid and 10 mM ammonium acetate [16]. The gradient program that was initially started at 35% B, was increased to 100% B in 3.5 min and then held at 100% B for 0.5 min, decreased to 35% B in 0.1 min, and then held at 35% B for 0.9 min, enabling a short runtime of 5 min. Chromatographic separation was performed using a reverse-phased UHPLC analytical column (Biocrates Life Sciences AG, Innsbruck, Austria) at 50 °C. Chromatographic performance was then enhanced using a SecurityGuard ULTRA Cartridge C28/XB-C18 for 2.1 mm ID precolumn (Phenomenex Cat. No. AJ0- 8782). An injection volume of 5 μL was used. Mass spectrometric detection was accomplished with electrospray ionization in negative ion mode. Two MRM transitions were used for each target bile acid for semi-quantitative evaluation [16,21].

2.9. Statistics

The metabolic data were analyzed by univariate and multivariate statistical methods. The sex- and day-stratified heteroscedastic t-test ("Welch test") was applied to compare metabolite levels of the different dose groups with respective controls for each matrix. For all the metabolites, changes were calculated as the ratio of the median of metabolite levels in individual rats in a treatment group to the median of metabolite levels in rats in a matched control group (time point, dose level and sex). These ratios are referred to as "relative abundance". The computations were performed using the standardized routines setup in Java and Oracle database, and the relative abundances, *p*-values and t-values were collected as metabolic profiles and made available through MetaMap®Tox [19].

The Principal Component Analysis (PCA) and Hierarchical Clustering Analysis (HCA) were performed in R Statistical Software [22,23]. Prior to computing PCA and HCA, the data were transformed to a log scale, centered by subtracting the mean of the control group and scaled by the respective standard deviation for each metabolite. Missing data were imputed using the nearest neighbor method implemented in function impute.knn from the package impute [24]. The metabolites missing in more than 20% of samples, and subsequently, the animals missing more than 35% metabolites were removed from the analysis. The HCA was performed at the level of a treatment group based on the mean values of each metabolite within a specific dose and sex group.

2.10. Bioinformatics

The Divisive Amplicon Denoising Algorithm (DADA) treats every sequence uniquely without clustering them, which proves advantageous as the variability of as small as one nucleotide is considered [25]. DADA2 v1.10 package was used to process the sequencing

data using a customized workflow [25]. A table of amplicon sequence variants (ASV) was obtained by denoising using a customized DADA2 v1.10 denoising workflow. The workflow includes quality control, primer removal, denoising, taxonomy assignments using RDP classifier and creation of a phylogenetic tree [26] (see Figure 2). Forward and reverse primers were trimmed from the raw reads using cutadapt [26]. As paired-end reads had to be used for further analysis, the reads or sequences were merged to about 415 bp length. Quality checking (QC) involved checking the read lengths and the quality of the joined reads. Taxonomy was assigned to ASV sequences using the Naïve Bayesian classifier implemented in DADA2 using the RDP database [27]. This resulted in the output in the form of a BIOM table with all the information regarding the sequences and abundances of ASVs and the assigned taxa information.
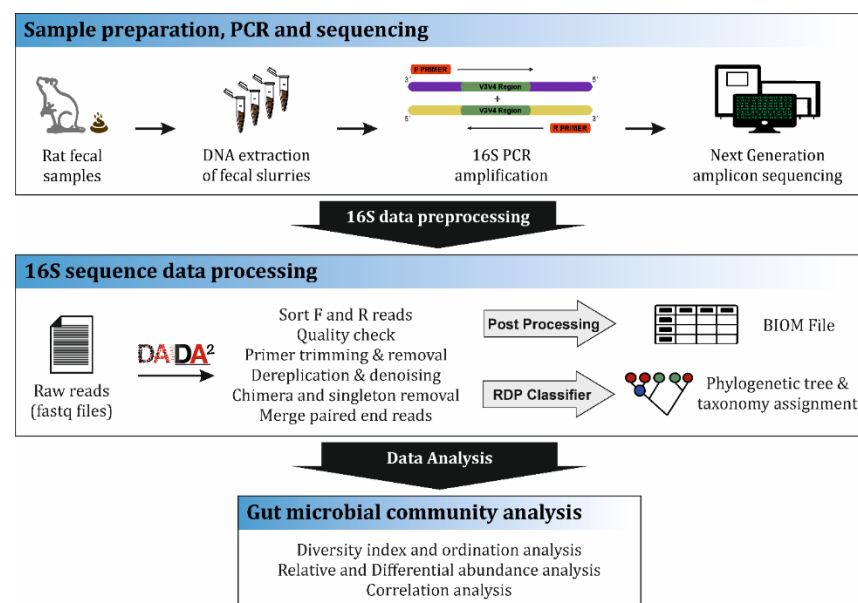

Figure 2. 16S community analysis workflow. The first step involved the preparation of fecal samples collected during necropsy (day 28) from the Wistar rats. Samples were subjected to DNA isolation, quantification and further 16S rDNA gene amplification by Polymer chain reaction (PCR) and sequencing report generation. The next step involved the data pre-processing where filtering, denoising and demultiplexing of the reads were conducted by DADA2 software and the final step was the bacterial community data analysis.

2.11. 16S Data Normalization, Diversity and Relative Abundances Analyses

The community analysis was conducted in R using RAM (Chen, Wen et al. "Package 'RAM'" (2018)), and DESeq2 packages [28]. The raw data were checked for completeness, and empty rows were removed. The BIOM table contained 2859,130 reads belonging to 31,023 ASVs from 198 samples. The raw reads were used for alpha diversity analysis using the group.diversity function in RAM package. As a part of data cleanup, ASVs or reads that did not have taxonomic assignment up to the family level were removed. Further, ASVs with non-zero counts in at least two samples were retained, and the others were removed, resulting in 2496,649 reads belonging to 1946 ASVs. These filtered data were used for relative abundance analysis. Stacked bars were plotted using RAM package to determine the relative bacterial abundances in the different antibiotic-treated rats. An additional stacked bar was plotted to estimate the group indicators, which indicate the core taxa that are specific to particular conditions. Parameters used for the group indicators are A = 0.975, B = 0.975, stat = 0.975, *p*-value = 0.001, where A refers to the probability that the animal belongs to a combination of conditions given that a taxonomic family is found and B refers to the probability of finding a bacterial family given that the animal belongs to a combination of treatment groups. Stat refers to the association between A and B.

Count normalization of the dataset and the differential abundance analysis was done using DESeq2 workflow (via Phyloseq) [29–31]. This procedure follows custom scripts from the DESeq2 package. The filtered and normalized data were used for beta diversity analysis and HCA. Principle Coordinate Analysis (PCoA) was carried out using phylogenetic (weighted UniFrac) and non-phylogenetic (Bray-Curtis) based distances.

For the DESeq2 model, study (experimental batch), sex and treatment (a compositive variable of administered compound and dose) were used as independent variables, with an additional interaction term for sex and treatment. The log2 fold change values of bacterial family that are significantly present or absent in a particular treatment relative to the controls were estimated. An additional feature to include batch effects in DESeq2 was performed to include any minor study-dependent variabilities. The differential abundance analysis allowed us to visualize the significant changes in specific bacterial families in their abundances in different treatments with respect to the controls. This also allowed us to visualize differences between the two dose groups and sexes. These log2 fold change values were then used for final correlation analysis with the metabolome data.

2.12. Correlation Analysis

In order to enable the comparison of the metabolome data to the microbiome data, log2 fold changes were calculated for the two metabolome matrices. The fold change matrices were used to compute correlations between different metabolites and 16S bacterial families using R. Pearson correlation analysis was performed for fecal bacterial families with plasma and feces metabolomes, respectively. A separate targeted measurement was performed for the bile acids in the low-dose groups. A similar correlation analysis was conducted for these low-dose treatments for the bile acid metabolites. A correlation test was performed to determine statistical significance. Only metabolites and bacterial families that had correlations with $p < 0.05$ and absolute strength of correlation >0.6 were retained.

3. Results

3.1. Clinical Signs

There were no mortalities in any of the treatment groups, except for one animal at the beginning of the study in the female group with Streptomycin treatment, which was not treatment-related. No clinical signs of toxicity were observed in any of the animals that received Lincomycin, Sparfloxacin, Streptomycin and Vancomycin. Animals treated with Roxithromycin showed slight salivation immediately after administration. The group of female animals treated with Clindamycin showed relevant clinical signs including salivation and semi-closed eyelid (four animals), and one of the animals showed piloerection. Similarly, males treated with Clindamycin showed slight salivation (all animals), semi-closed eyelid (three animals) and, two of them were in poor condition. Except for salivation, these findings were only observed in the individual animals on 1–3 days of the administration period out of 28 days. Therefore, and in the absence of body weight effects, these observations were assessed as borderline effects indicative of marginal systemic toxicity of Clindamycin at 200 mg/kg body weight. Relative changes in body weight and food consumption noted upon administration of the test compounds are shown in Supplementary Table S1. Treated animals did not present any significant changes with respect to body weight when compared to the controls for both males and females.

3.2. Diversity Analysis

Shannon true diversity of the fecal microbiome of all the six antibiotic treatments and restricted-diet-fed rats was compared to controls for both dose groups and sexes (Figure 3). Shannon true diversity indicates the diversity of different bacterial taxa present in a specific treatment [32]. The larger the boxes in the boxplot, the higher is the variability between the individual samples of a specific group/condition. The dots falling outside the boxes are outliers. A clear reduction in the diversity in the samples of all the antibiotic treatments was noted. Control animals had higher inter-individual variability in both

the sexes compared to antibiotic-treated animals. The higher the diversity, the higher the presence of different bacterial taxa, which is highest in the controls, followed by the restricted-diet-fed animals. Among the different antibiotic treatments tested, samples from Streptomycin-treated animals retained a relatively high diversity in bacterial taxa for both males and females compared to the other antibiotic-treated animals. Sparfloxacin and Vancomycin treated animals showed the least diversity in both the sexes. Overall, dose dependency was not very apparent and was quite marginal in both the sexes, with a possible exception of Streptomycin. Using the diversity information, the Shannon evenness boxplot was plotted (see Figure S1).
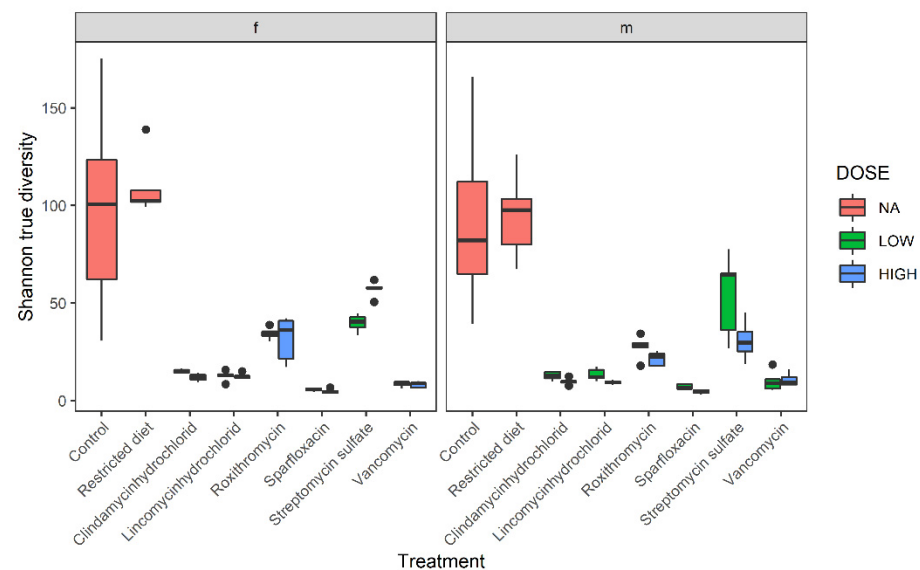

Figure 3. Shannon true diversity analysis of six antibiotic treatments, restricted-diet-fed and controls for both male and female Wistar rats. Boxplot shows the diversity analysis on the left for females (f) and on the right for males (m). The colors show different dose groups, where red refers to no dose applicable, blue box refers to high-dose and green refers to low-dose groups. The x-axis shows the different treatment groups, and y-axis shows Shannon diversity value; whiskers denote standard deviations, solid lines within the boxes indicate the group median and dots lying outside the boxes are outliers. A closer comparison of the treated groups and dose response is depicted in Supplementary Figure S9.

Consistent with the Shannon true diversity index, the Shannon evenness profiles of the antibiotics again showed a very marginal dose dependency for both sexes except for the Streptomycin treatments.

Following the alpha diversity analysis, a beta diversity analysis using two different distance matrices was conducted. One was a rank-based Principle Coordinate Analysis (PCoA) using a non-phylogenetic distance matrix called the Bray–Curtis distance. The second one was a phylogenetic-based distance matrix called Weighted UniFrac distances. Figure 4a depicts the non-phylogenetic distance-based rank PCoA analysis of the bacterial taxa present in different conditions. The PCoA was also used to observe any exclusive sex-based clustering. Six clear clusterings of the different treatments could be observed. We observed one cluster with controls, restricted-diet-fed and Streptomycin treated animals; a second with Roxithromycin, Sparfloxacin, Vancomycin; and two clusters formed by the lincosamides treated groups. In addition to the four clusters, two different yet closely located clusters of the two lincosamide treatments (Clindamycin and Lincomycin) were evident. Thus, the Streptomycin treatment showed the same results as in the diversity analysis; i.e., it appeared to be more similar to the controls than to any other antibiotic treatment.
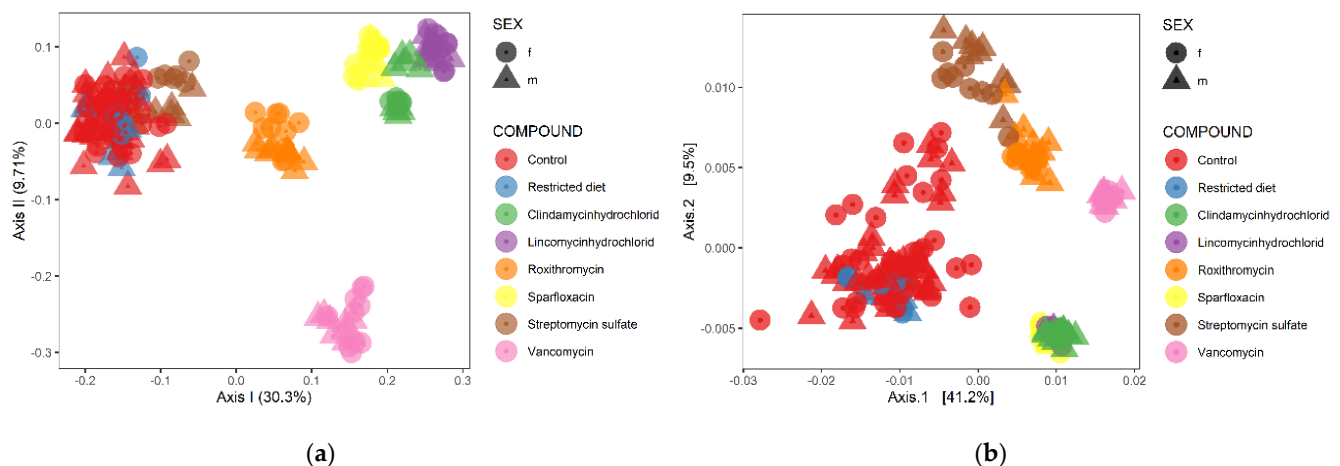
Figure 4. Principle Coordinate Analysis (PCoA) of bacterial families from different treatments. (**a**) The distance matrix used is Bray–Curtis, which is a rank-based clustering. (**b**) Principle Coordinate Analysis (PCoA) using weighted UniFrac distance matrix that is a phylogenetic-based distance that takes bacterial abundances into account.

Sex-dependent clustering could not be observed in any of the treatments, whereas a clear antibiotic class dependency was evident. Further, a phylogenetic distance-based beta diversity analysis demonstrated changes as shown in Figure 4b. Consistent with our previous Bray–Curtis-based PCoA analysis, the weighted UniFrac distance matrix produced six visible clusters. The samples from animals belonging to controls and restricted diet formed a cluster together in the phylogenetic distance-based matrix, similar to the Bray–Curtis distance matrix. Similarly, treatments of two lincosamides, Clindamycin and Lincomycin, clustered together and with Sparfloxacin treatments, whereas Streptomycin, Roxithromycin and Vancomycin treatment groups clustered separately from others. As this analysis involves phylogenetic associations between the bacterial taxa, the clusters at some points appear to converge with nearby associated clusters, showing homology in their relations. This also explains a large spread in the control and Streptomycin treatments and closeness of Sparfloxacin treatments to the lincosamides cluster.

3.3. Hierarchical Clustering Analysis

The hierarchical clustering of gut (fecal) bacterial families based on both sexes and dose groups is shown in Figure 5. Control data from all four selected studies have been combined. The hierarchical clustering showed clear antibiotic-specific clustering, consistent with what was observed in the beta diversity analysis. A heatmap was generated with hierarchical clustering (HC) of not only the different treatments (taking every single sample into account and not means or medians) or conditions but also the bacterial families. Potential co-occurrences of bacterial families are shown in Figure 5. As dose and sex did not contribute very much to the changes in the microbiome, they were combined for the analysis. Streptomycin treated animals clustered closely with controls, whereas Vancomycin-treated animals clustered the farthest from the control cluster. Restricted-diet-fed animals merged together with the control cluster, whereas five clear antibiotic-based clusters could be observed. Both lincosamides—Clindamycin and Lincomycin—clustered together, showing an antibiotic class-based effect.

Figure 5. Hierarchical clustering analysis of 16S bacterial families in different treatments, dose groups and sexes. Heatmap showing occurrences of bacterial families in different antibiotic treatment groups, including hierarchical clustering of bacteria families and different treatments. Color coding on the right indicates the different treatment groups that correspond to the clustering analysis on the left. The black bands on the right show the samples from individual animals belonging to respective treatment groups. Dose groups and sexes showed very marginal differences; hence, they were not separated.

The black bands on the right side of the figure represent the respective treatment that the bands correspond to. The bacterial families could be observed taking inter-individual variations into account. The presence or absence of some of these bacterial families like *Paenibacillaceae*, *Bacillaceae* and *Eubacteriaceae* also distinguish between the two lincosamides as they occur in Lincomycin- and not Clindamycin-treated animals. Families like *Anaeroplasmataceae* and *Deferribacteriaceae* were specific to only Vancomycin treatments compared to all the other treatment groups. Roxithromycin treatments shared some bacterial families including *Rikenellaceae* and *Eubacteriaceae* with Strepmycin treatments and controls. Sparfloxacin showed the highest abundances of specific families like *Bifidobacteriaceae* and *Coriobacteriaceae* families that could not be observed in such high abundances in any of the other treatment groups. Finally, the *Lachnospiraceae* family was prevelant in all the treatments and the controls except for Vancomycin-treated animals. Families like *Ruminococacceae* and *Erysipelotricaceae* were observed in all the treatment groups followed by *Lachnospiraceae* and *Verrucomicrobiaceae*, which were also present in all the treatment groups although varying in abundances. HC does not show any sex- or dose-based grouping, which means low dose (LD) selection was enough for the influencing alterations. Overall, the heatmap shows the clustering of not only the different treatments but also the 16S-analyses-based bacterial families.

3.4. Relative Abundance Analysis

Relative abundance analysis is presented as a stacked bar graph (Supplementary Figure S3), where every color depicts one bacterial family. The inter-individual variability could be clearly observed in all the conditions. Antibiotic treatments portray occurrences of bacterial families significantly differently compared to the controls, with the exception of Streptomycin-treated animals, which is consistent with respect to diversity analyses,

showing that the influence of Streptomycin on fecal microbiome communities is rather minor such that this group shows similar bacterial abundances as the restricted diet and control groups. Clindamycin- and Lincomycin-treated animals behaved fairly similarly with greater abundance of the *Ruminococcaceae* family than any other treatment group. Both the lincosamides showed the maximum abundance of *Firmicutes* phyla amongst all the other treatment groups. A very marginal dose- and sex-specific variation in the bacterial abundances could be observed. Roxithromycin showed a very high abundance of *Rikenellaceae* compared to any other treatment. Vancomycin-treated animals were observed to have the highest abundance of *Enterobacteriaceae*, which could only be seen in the two lincosamide treatment groups and likely in no other. Similar to Sparfloxacin, the Vancomycin treatment group showed more than 50% contribution of *Verrucomicobiaceae* in the total abundance. *Enterobacteriaceae* family could be observed to be specific to Vancomycin and two lincosamide treatments (Supplementary Figure S3).

Group indicator analysis gives the relative abundances of the taxonomic groups, which are statistical indicators of the experimental conditions (different treatments, in our case). The families shown in Figure 6 show fidelity, specificity and association strength of 0.975. This means that core bacterial families that are specific to a condition or a combination of conditions have been shown here. Group indicators are derived from the likelihood of finding a specific bacterial family in a specific treatment. Figure 6 also shows clear inter-individual variability in the group indicator appearances. A very clear inter-individual variability can be observed in the stacked bar plot. The core bacterial families that have high contributions in a particular treatment group have a value of about 1 or closer. Antibiotic-specific core bacterial families can be observed. The animals in the Streptomycin treatment group showed group indicators highly similar to the controls and restricted diet-fed animals. However, unlike controls and Streptomycin groups, the restricted diet group of animals showed an increased abundance of the *Lactobacillaceae* family. This is consistent with the previous findings that caloric restriction promotes increased growth of Lactobacillus species in rat fecal microbiota [33]. *Verrucomicrobiaceae* was not a core bacterial family in Roxithromycin and lincosamide treatments compared to other treatment groups where they contributed as a core bacterial family. Clindamycin- and lincosamide-treated animals showed high contributions of *Enterobacteriaceae* followed by *Erysipelptrichaceae* families, demonstrating antibiotic-class-specific changes. Roxithromycin treatments possessed the highest abundance of the *Rikenellaceae* family, which could not be observed in any of the other treatments. Similarly, contributions of *Lachnospiraceae* family were observed in all the treatments except for Vancomycin treatment. Overall, antibiotic-specific core bacterial families could be observed well from the analysis.
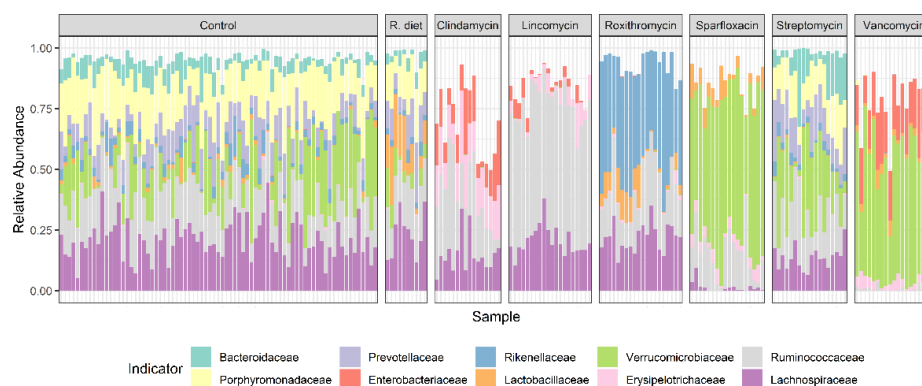

Figure 6. Stacked bar showing group indicators or core bacterial families that were detected in specific treatment groups, where R. diet refers to the restricted diet (−20%) group. Individual animal variability can be easily observed. Dose groups and sexes showed very marginal differences; hence, they were not separated. Antibiotic treatments clearly show class-dependent effects on the intestinal community composition. Compared to control, restricted diet and Streptomycin sulfate treatment groups, all the other antibiotics produced reduced/changed bacterial diversity and richness.

3.5. Differential Abundance Analysis

Differential abundance analysis was carried out using DESeq2 package, which is used to identify specific bacterial taxa (or families in our case) that are associated with specific treatments. This helps to understand more about specific bacterial families which are significantly abundant or rare in specific treatments compared to the controls. This provides more insight regarding the role of such specific bacterial taxa and eventually their influence in the metabolic activities of the different antibiotic-treated Wistar rats. Models were created for each treatment for each dose group and sex. This analysis was conducted in order to estimate the fold changes of significantly altered bacterial families in different treatments relative to the controls. This fold change information from DESeq2 analysis is further used for correlation analysis in order to compare with the fold changes of different metabolites in the three matrices. The results of this analysis are shown as scatter plots; see Supplementary Table S16, where each dot indicates individual read/amplicon sequence variant (ASV) belonging to a specific bacterial family.

Streptomycin LD treatments versus controls for both the sexes (females to the left and males on the right) can be used to observe the specific bacterial families, such as *Ruminococcaeceae*, few ASVs that belong to this family of bacteria are present in almost 30 log2FC, and others were very less in abundance compared to control animals. This is the reason why the log2 fold change for most of the ASVs belonging to *Ruminococcaceae* family, as shown in Table S16, has a highly negative value when differential abundance analysis was conducted for female rats. *Eubacteriaceae* family could be observed to be present in very high abundance compared to controls in Streptomycin-treated female rats. Similarly, in males, many differentially abundant families could be observed similar to females. *Eubacteriaceae* family could be observed to be present abundantly in males treated with Streptomycin compared to controls, and ASVs belonging to families like *Lachnospiraceae* and *Ruminococcaceae* were present in very high abundance and also low compared to controls. Other families including *Rikenellaceae*, *Sutterellaceae* and some others were present in lower abundance compared to controls for both sexes.

For the two different antibiotic treatments, only low-dose groups from both females and males have been depicted in the scatter plots; for the complete data of differential abundance scatter plots for all the LD treatments, see Supplementary Table S16. As differential abundance analysis for LD and HD only marginally differed, only the LD plots are shown in order to avoid overloading of redundant data. In Vancomycin LD treatments (see Table S16), not much difference could be observed between the males and females with respect to the differential abundance analysis, except for *Anaeroplasmataceae* family, in which it was observed in higher abundances in females than males. In both the sexes, *Enterobacteriaceae* and *Verrucomicrobiaceae* families were very high in abundance compared to control animals. Most of the other represented bacterial families were observed in reduced abundance compared to controls in both the sexes. These results showed how rarely or abundantly certain families are present when there is a lack of nourishment. The results from this analysis were consistent with what was observed in the heatmap of hierarchical clustering analysis.

3.6. Metabolome Data Analysis

3.6.1. Fecal Metabolome

A hierarchical clustering analysis was conducted for all the measured metabolites from the fecal samples of the controls and different treatments. The dendrogram in Figure 7a shows the clustering based on Euclidean distances of all the treatments and controls, based on sex and dose groups. Control groups from the four studies were combined into two, separating males and females. The clustering showed a very similar pattern as it was observed in the 16S clustering. Treatment-dependent clustering could be clearly observed. Controls and restricted-diet-fed animals had very similar fecal metabolome profiles, as they were observed to be closely clustered. Streptomycin- along with Roxithromycin-treated animals clustered the closest with each other and to controls compared to the other

tested drugs. In Roxithromycin and Streptomycin treatment groups, a sex-based clustering could be observed in the dendrogram. Animals treated with the two lincosamides, Clindamycin and Lincomycin, clustered very closely but also had marginal differences between them. Clindamycin treatment group showed a dose-dependent clustering, which could not be observed for any of the other drugs. Closest to the lincosamides were samples from Sparfloxacin-treated animals. Vancomycin-treated samples showed the most distant clustering with respect to the controls. A Principal Component Analysis using the same data showed a very consistent observation (see Supplementary Figure S4). Similarly, HCA and PCA analysis of cecum metabolome data was carried out and can be found in the supplementary data (see Figures S5 and S6, respectively). Both the analyses result in similar and comparable clustering.
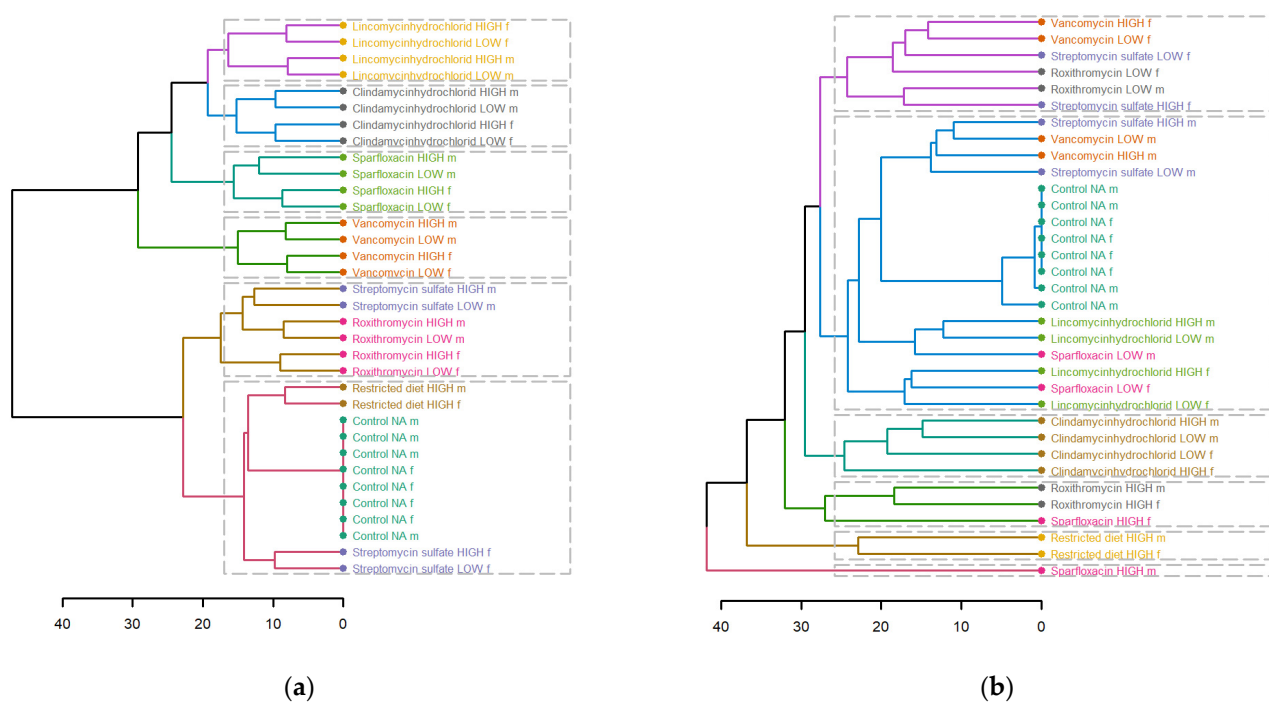

Figure 7. Dendrogram showing hierarchical clustering of (**a**) fecal and (**b**) plasma metabolites of different treatments, dose groups and sex. Euclidean distance was used, and different treatments are depicted, and different colors and dotted boxes show different clusters.

3.6.2. Plasma Metabolome

The dendrogram shown in Figure 7b shows the clustering of plasma metabolomes of controls, restricted-diet-fed and six antibiotic treatments. The clustering showed restricted-diet-fed samples to be very different from the controls, in sharp contrast to the observations made in the fecal or cecal metabolome (see Figure S5 for cecum metabolome HCA analysis) and microbiome clustering analysis. Sparfloxacin- and Roxithromycin-treated animals showed a dose-dependent clustering, which could not be observed in any of the other antibiotic treatments. Vancomycin treatment showed a big separation based on gender. Samples from animals treated with the two lincosamides, Clindamycin and Lincomycin, also showed a profound difference in their plasma metabolome profiles. Overall, the analysis showed far less treatment-based clustering than in the fecal and microbiome analysis. The exceptions being restricted diet feeding and the Clindamycin treatments, which formed neat clusters.

3.6.3. Controls vs. Restricted Diet in Plasma and Fecal Matrices

Restricted-diet-fed animals showed no significant differences compared to evaluate similarity. There was, however, a huge difference in the plasma metabolome, which makes

it interesting to conduct an ordination analysis only using restricted diet and control data. When a PCA was prepared using the fecal metabolome data (see Figure 8a), the restricted diet treatments did not form a cluster different from the controls along Principle components (PCs) 1 and 2; however, they clearly separated along PCs 2 and 3.
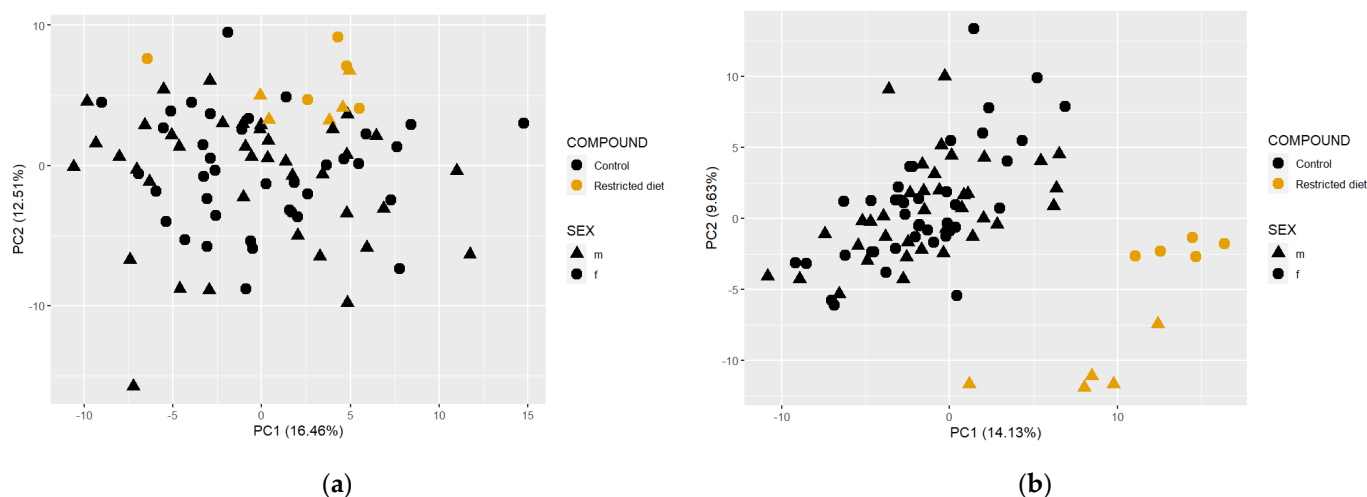

Figure 8. Principal component analysis (PCA) of restricted-diet-fed and controls from all the studies. (**a**) PCA using feces metabolome (left side); (**b**) plasma metabolome data (right side).

Further, when the same was done using a plasma metabolome data (see Figure 8b), a clear separation could be observed on the first principal component, between the controls and the restricted diet. This showed a clear influence of reduced nourishment on the plasma metabolome of the rats, which could not be observed in other matrices and in the gut bacterial community composition. This indication clearly means that the difference in the plasma metabolome of the 20% reduced diet does not come from the gut microbiome but the diet of the host itself.

Metabolome data from plasma, fecal and cecum could be compared from our results, and very marginal differences between fecal and cecum metabolome were observed, whereas the plasma metabolome differed significantly from the other two. The microbiome data showed very consistent clustering compared to feces and cecum metabolome profiles. The HCA analysis of microbiome data can be found in Supplementary Figure S2. The concordant findings prove the comparability of the two datasets. Restricted-diet-animals had similar gut microbial composition and fecal and cecum metabolome profiles as controls but showed differences in the plasma metabolomes. Compared to all the antibiotics, samples from animals treated with Streptomycin showed the least differences in microbiome and fecal metabolome profiles compared to the controls, and those from the Vancomycin treated group showed the highest. The two lincosamides-treated animal groups showed a very marginal influence on both microbial composition and fecal metabolome, showing an antibiotic class-dependent effect. After Streptomycin, Roxithromycin treatment groups showed the highest similar influence of microbiome and fecal metabolome compared to the controls.

3.6.4. Comparison between Plasma, Feces and Cecum Metabolome Profiles

Cecum and fecal metabolomes were compared to observe the number of overlaps or contrasts between the different matrices. Pearson correlation was conducted to compare the different metabolome matrices to understand the similarities or differences between them (see Supplementary Figure S8). A boxplot graph was prepared to analyze the Correlation coefficients of feces vs. cecum matrix, plasma vs. cecum and plasma versus feces metabolomes (Supplementary Figure S8). The figure shows the highest correlations between feces and cecum metabolomes compared to others, with a correlation coefficient

value as high as 0.7 approximately. Whereas, cecum versus plasma matrix and feces versus plasma matrix were almost near 0, indicating the least comparability between plasma metabolome with both feces and cecum metabolomes. There were although some biomarker metabolites observed, that belonged to metabolites like indole-3-acetic acid and allantoin that showed highest correlations between the plasma and feces and cecum metabolome (see Supplementary Figure S8).

Cecum and feces metabolomes showed very high similarity. A diagonal line in the heat map shows the similarities between the metabolites that are in common between the two matrices. The straight line shows highly significant correlations between the cecal and fecal metabolites, proving the very slightly marginal difference between the two matrices. This result supports the concept of using feces as a matrix that can be obtained using non-invasive methods, and it also promotes a longitudinal study design (also known from Behr et al., 2018, comparing different gut tissue matrices). However, when plasma metabolome was compared with fecal and cecal metabolomes, very low correlations could be observed between plasma and the two matrices. Plasma metabolome appears to be an entirely different matrix compared to both feces and cecum based on its metabolite composition. With this, we hypothesize the potential reason could be that plasma metabolome comprises a crosstalk between the host and gut-mediated metabolites, as also known from Behr et al., 2018 [15]. Not only gut and host metabolites, but also co-metabolites could be found in plasma; hence, it would pose as an entirely different matrix compared to feces and cecum.

3.7. Correlation Analysis

Inter-omic Pearson Correlation was conducted to compare the log2fold changes of significantly altered metabolites in all the three matrices compared to bacterial families, for all the treatments. The log2fold change values were calculated for all the treatments relative to the controls using DEseq2. These fold change values for every treatment were compared between the metabolome and microbiome profiles. Some metabolites are present in multiple numbers due to their different types of mass spectrometry measurements (LC or GC). In all three matrices, it was observed that the majority of the bacterial families correlated strongly with the amino acids, lipids and related metabolite classes. Compared to plasma metabolome, feces metabolomes showed a higher number of correlations between the bacterial families and respective metabolites.

3.7.1. Feces Matrix

The correlation analysis between two omics datasets shows the relationship between the presence/absence of a particular gut bacterial family with the presence/absence of a specific fecal metabolite (see Figure 9). The complexity of changes, relative to the number of antibiotics employed, however, did not allow us to exactly identify individual metabolite–microbiome connections. For those fecal metabolites that we altered by the treatment the correlation analysis heat map does show how strong these are correlated (positively and/or negatively) with the gut bacterial families Out of 39 annotated bacterial families, only 12 were found to possess the strongest correlations with feces metabolite levels. The resulting strength of the correlation or the value of the correlation coefficient is governed by the cumulative relative changes of bacterial taxa/fecal metabolite in all the treatments with respect to controls. The stronger the correlations are (irrespective of the direction), the more chances are that they originate from all the treatments. A strongly positive correlation (red box) indicates that both the metabolite and bacterial family change in the same direction (either both are strongly upregulated or strongly downregulated), while the strongly negative (blue box) indicates an inverse correlation, meaning if the metabolite level increases, the fold change of the corresponding bacteria family must decrease and vice versa. To evaluate inter-treatment effects, one can go back to the DESeq2 data to refer to changes in the bacterial families in respective treatments and to metabolome profiles to refer to changes in different metabolite concentrations.

Figure 9. Pearson colorations of 16S bacterial families and corresponding fecal metabolite classes. The heatmap shows positive (red) and negative (blue) correlations between fecal metabolites and corresponding bacterial families. Metabolite classes have been indicated along with the metabolite names on the horizontal part of the figure. Black dots within the boxes indicate *p*-value < 0.05 calculated using cor.test.

Most of the amino acids such as arginine, histidine, alanine, valine, phenylalanine, glycine, asparagine, serine, glutamine, methionine and threonine show predominantly negative correlations with the bacterial families (Supplementary Figure S9). Only about 3-5 bacterial families from the list of 12 families positively correlate with these amino acids. Amino acids like glycine, valine and leucine are positively correlated with families *Verrucomicrobiaceae*, *Anaeroplasmataceae* and *Lactobacillaceae*, which belong to Verrucomicrobia, Tenericutes and Firmicutes phyla, respectively. *Lactobacillaceae, Verrucomicrobiaceae* and *Anaeroplasmataceae* form clusters of highly positive correlations with amino acids such as glycine, leucine, isoleucine, phenylalanine, alanine, valine and proline, suggesting common functions between these bacterial families.

Tryptophan, being one of the most important products from dietary source and endogenous bacterial metabolism, correlates negatively with a majority of bacterial families except for *Rikenellaceae* that correlates towards the positive direction in the feces matrix. Ornithine, which is well known to result from gut bacterial metabolism, also appears to have profoundly negative correlations with the gut bacterial families, with only 3–4 exceptions, including *Rikenellaceae, Porphyromonadaceae* and *Eubacteriaceae* (See Figure S9). Most metabolites involved in energy metabolism show few strong correlations, irrespective of the direction, whereas 2-hydroxyburyrate and 3-hydroxyburate have some strongly negative correlations with bacteria belonging to mostly Bacteroidetes followed by Firmicutes and Proteobacteria phyla. One of the several gut-microbiomes-associated biomarkers, indole-3-acetic acid, appears to have slightly weak correlations irrespective of the direction, with the majority of the bacterial families except for three bacterial families *Verrumicrobiaceae, Anaeroplasmataceae* and *Ruminococcaceae*. Moreover, certain metabolites belonging to carbohydrates and related classes like lysine and glucuronic acid have mainly strong negative correlations, except for four bacterial taxa, namely, *Porphyromonadaceae, Rikenellaceae, Verrucomicrobiaceae* and *Anaeroplasmataceae* families (as shown in Figure 9).

Bacterial families *Verrucomicrobiaceae* and *Anaeroplasmataceae* have a very similar correlation, where they mostly positively correlate with the majority of fecal metabolites. Metabolites like hexadecanol, octadecanol and dodecanol that belong to complex fatty acids and lipids and related class have positive correlations with the majority of the bacterial families except for *Rikenellaceae*, for which the correlations are very weak. Clusters of positive correlations between specific bacterial families, including *Porphyromonadaceae, Ruminococcaceae, Lachnospiraceae, Bacteroidaceae, Prevotellaceae, Bdellovibrionaceae* and *Peptococcaceae,* could be observed with metabolites belonging to lipids, fatty acids and related classes, suggesting common functions between these bacterial families. Overall, most correlations between the intestinal bacteria and fecal metabolites belong to amino acids, lipids and fatty acids and energy metabolism-related metabolites.

A correlation analysis for 16S bacterial families and the bile acid pool from feces was carried out, and numerous correlations were observed irrespective of the direction (see Figure 10). Cholic acid, a primary bile acid, showed a negative correlation with the majority of bacterial families except for *Anaeroplasmataceae* and *Lactobacillaceae*, which belong to Tenericutes and Firmicutes phyla, respectively. *Ruminococcaceae* showed the strongest negative correlations with five taurine-conjugated bile acids, namely TCA, TMCA (both α and β), TCDCA and TUDCA. Two other taurine-conjugated bile acids, TDCA and TLCA, showed a completely different correlation in comparison, as they correlate positively with all the bacterial families listed except for two, *Lactobacillaceae* and *Peptostreptococcaeceae*. Unconjugated secondary and tertiary bile acids that cluster the closest to each other, such as MCA (both α and β), HDCA, DCA and LCA, strongly and positively correlate with the majority of the 16S bacterial families except for *Anaeroplasmataceae*. A glycine conjugated bile acid GCA shows positive correlations only with the bacterial families *Lactobacillaceae*, *Peptostreptococcaceae* and *Anaeroplasmataceae* compared to other bacterial families. Overall, four taurine-conjugated bile acids clustered together and show similar correlations with bacterial families, and unconjugated secondary and tertiary bile acids also clustered together and behaved similarly with respect to their correlations with bacterial families.

3.7.2. Plasma Matrix

Inter-omic correlations between the plasma metabolites and 16S bacterial families were less profound and not as many as between the fecal matrix and 16S bacterial families (see Figure 11). Out of 39 bacterial families, only 9 showed correlations with plasma metabolites. Similar to previous results, most of the correlated metabolites belonged to lipids and related classes, but also energy metabolites and amino acids and related metabolites. Lipids, fatty acids and derivatives like lysophocpohatidylcholine, linolenic acid, and phosphatidylcholines strongly positively correlated with specifically the *Bdellovibrionaceae* family compared to all the other bacterial families (see Figure 11). Other metabolites like 3-hydroxyindole were mostly positively correlated with all of the nine bacterial families, including the strongest positive correlation with *Ruminococcaeceae*. Creatine and creatinine strongly correlated in the negative direction particularly with four bacterial families, which are clustered very closely to each other in the dendrogram, namely *Ruminococcaceae, Bdellovibrionaceae, Lachnospiraceae* and *Peptostreptococcaceae*. Plasma metabolome does not only house gut-microbiome-associated metabolites but a variety of host metabolites and co-metabolites as well. Plasma reflects a huge crosstalk of metabolites resulting from different sources (like nutrition, microbial metabolism); hence, it is obvious to attain very limited or only a handful of correlations between these metabolites and the gut bacterial families, compared to the feces. As observed in Figure 11, one of the key metabolites known to have an influence on the gut microbiome-mediated metabolism, Indole-3-acetic acid (IAA), is observed to have a few strong correlations. One of the strongest and negative correlations of IAA was with *Anaeroplasmataceae* family. Carbohydrates and related metabolites including hexoses produced mainly strong positive correlations with a majority of the bacterial families, except for *Rikenellaceae* (as shown in Figure 11).

In contrast to feces, most correlations observed between the plasma bile acids and 16S bacterial families are positively correlated, with a few exceptions (see Figure 12). Primary bile acids clustering close to each other, cholic acid and CDCA mostly produced positive correlations with all ten of the 16S bacteria families. Glycine-conjugated bile acids GCA, GCDCA and also GDCA show a very similar trend with the majority of positive correlations with most 16S bacterial families with the difference in correlations with two bacterial families *Bacteroidaceae* and *Eubacteriaceae*. GCA and GCDCA showed negative correlations, while GDCA showed positive correlations with the two previously mentioned bacterial families. Among the taurine-conjugated secondary and tertiary bile acids, TLCA and TDCA showed a similar behavior in contrast to TCA and TMCA (both α and β). TLCA and TDCA showed positive correlations with all the ten bacteria taxa, while TCA and TMCA (both α and β) possessed the majority of negative correlations except for the *Eubacteriaceae* family. For unconjugated bile acids, although they formed separate clusters, MCA (both α and β), LCA and DCA showed comparable correlations with the bacterial associates. Additionally, other plasma biomarker metabolites such as 3-indoxylsulfate showed predominantly positive correlations, including the strongest positive correlations with the *Ruminococcaeae* family.
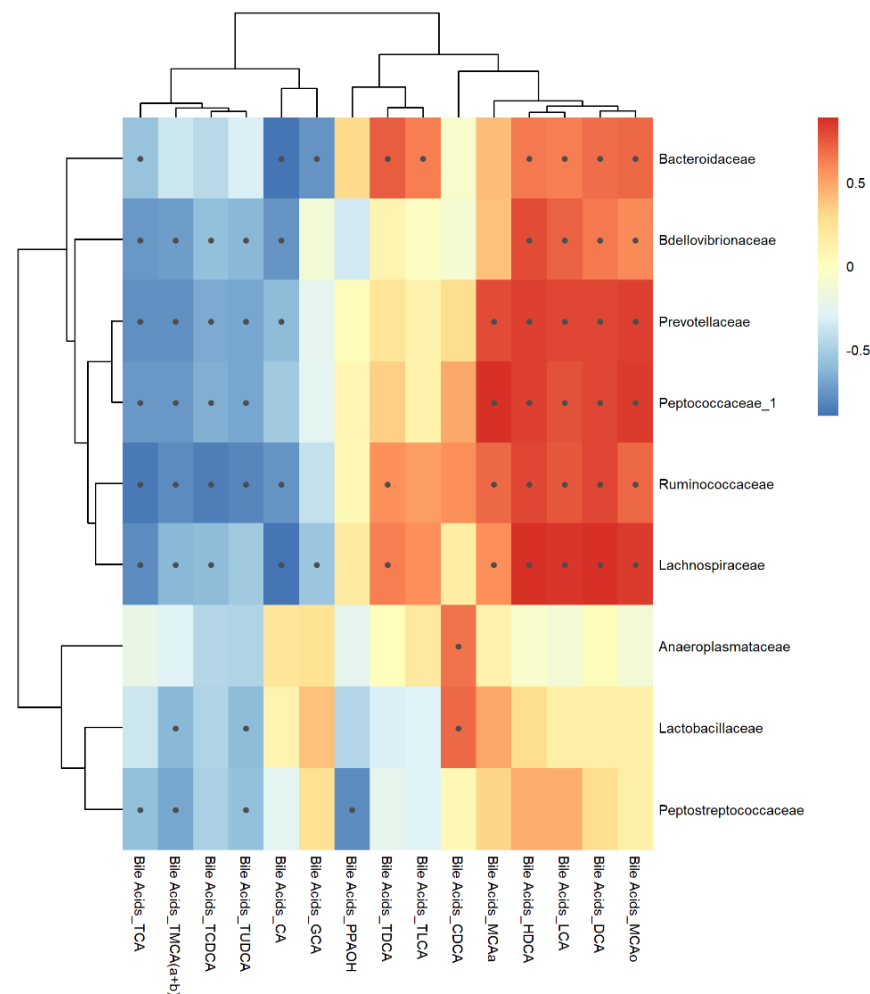
Figure 10. Inter-omic Pearson correlations between 16S bacterial taxa and bile acid metabolites measured from feces. Black dots within the boxes indicate *p*-value < 0.05 calculated using cor.test.
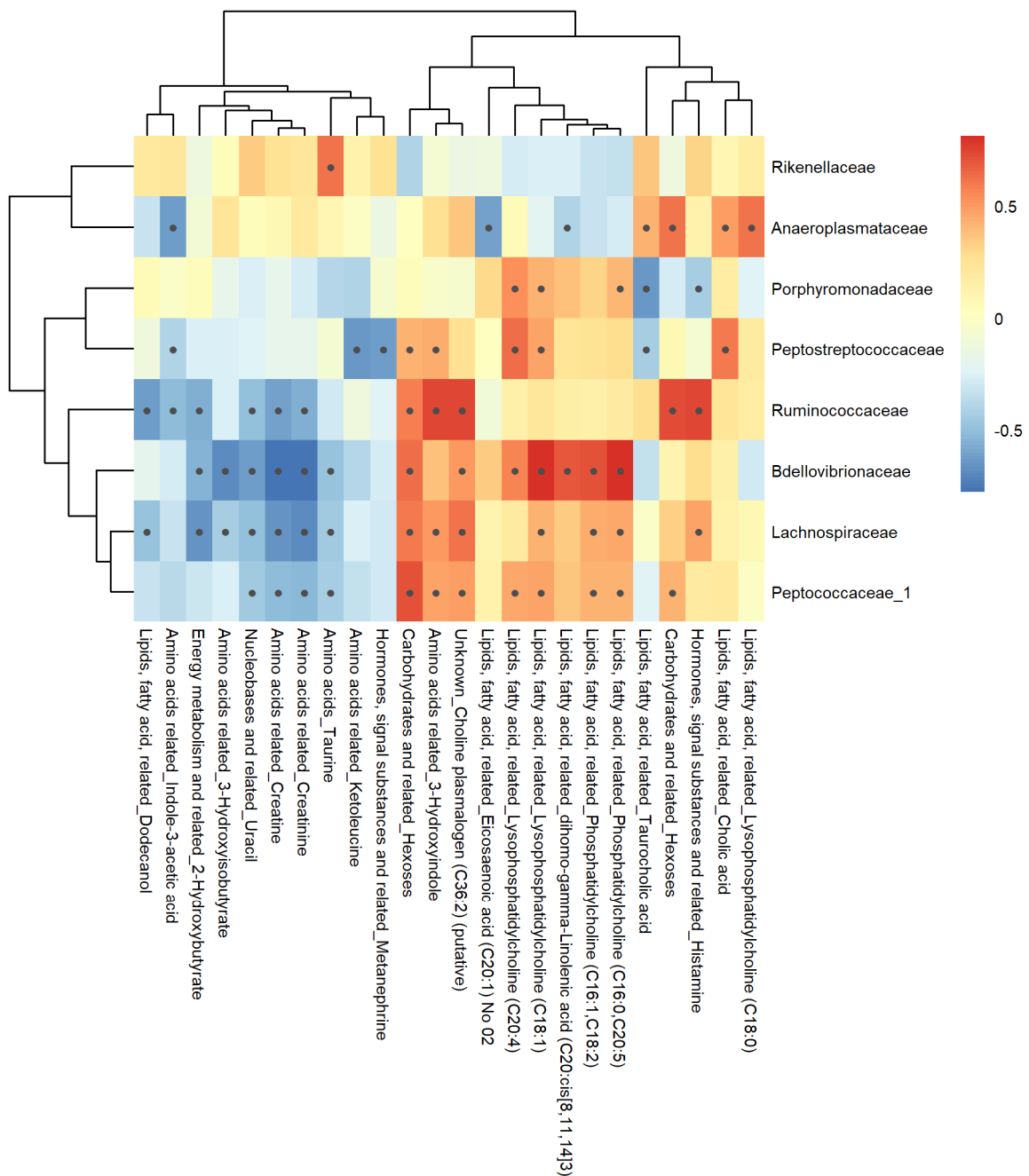
Figure 11. Pearson correlations of 16S bacterial families with plasma metabolite classes. The heatmap shows positive (red) and negative (blue) correlations between plasma metabolites and corresponding bacterial families. Metabolite classes have been indicated along with the metabolite names on the horizontal part of the figure. Black dots within the boxes indicate *p*-value < 0.05 calculated using cor.test.
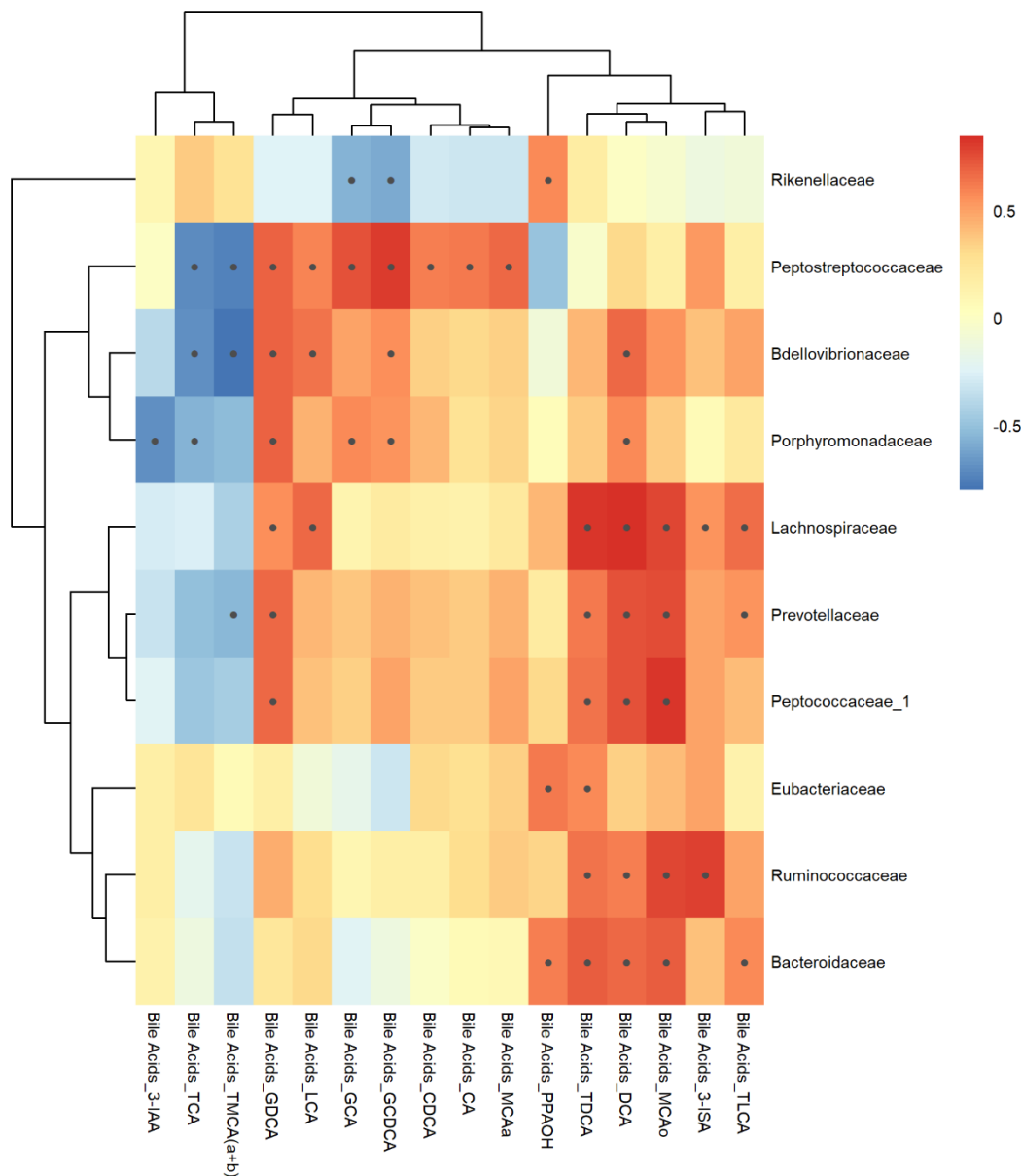
Figure 12. Correlation analysis using Pearson correlations between plasma bile acids and 16S bacterial families. Black dots within the boxes indicate *p*-value < 0.05 calculated using cor.test.

4. Discussion

The aim of this study was to understand the correlation between microbiome, fecal and plasma metabolomes. Our analysis now provides a connectivity map that shows how microbiome communities are responsible for the formation of fecal metabolites and how these are connected with the plasma metabolome.

4.1. Microbiome Analysis

Antibiotic class-specific effects on the gut bacterial composition in Wistar rats could be clearly and consistently observed in diversity and relative abundance analyses. The least effective antibiotic in changing microbiome communities was Streptomycin sulfate. This is not entirely surprising as Streptomycin has its primary antibiotic action on the aerobic microbiome, whereas most of the facultative anaerobes that dominate the gut are resistant to this antibiotic [17]. Treatment with Roxithromycin, affecting Gram-positive bacteria and some Gram-negative bacteria [17], produced the second least compositional

changes in the gut microbiome. In contrast, Vancomycin produced profound changes in the gut microbiome, which is concordant to its broad bactericidal activity against Gram-positive organisms [17]. Animals treated with the lincosamide antibiotics Clindamycin and Lincomycin, showed very similar changes in bacterial communities, demonstrating a clear antibiotic class-dependent effect as they are selectively effective against staphylococci, streptococci and most anaerobic bacteria [34]. Dose-response was marginal for all antibiotics, with the exception of Streptomycin, indicating that the low doses were high enough to elicit gut dysbiosis. Sex-based differences at a family level were overall also marginal. However, it should be noted that at a species-level, at least in humans, sex-specific differences in microbiome communities have been described [34–36]. Dose-response was marginal for all antibiotics, with the exception of Streptomycin, indicating that the low doses were high enough to elicit gut dysbiosis. Sex-based differences at a family level were overall also marginal. However, it should be noted that at the species level, at least in humans, sex-specific differences in microbiome communities have been described [35,36]. The PCA analysis using phylogenetic distance clustering was in- line with the above-mentioned conclusions drawn from the Shannon index. Shannon diversity indices have two major components: the number of species present (or species richness) and their relative abundances (or species evenness). The latter showed that Vancomycin and Sparfloxacin treatments have the least even composition compared to all the others, irrespective of the dose groups and sex. Both antibiotics are known to have a broad-spectrum activity against Gram-negative and Gram-positive microorganisms [37]. This explains why we observed the least diverse and highly uneven (less dominant) bacterial taxa present in these two treatment groups.

Relative abundance analysis showed on individual animal levels a clear inter-individual variability. From a birds-eye perspective, treatments can be readily identified as such; nevertheless, the samples from control animals possess such a recognizable variability of relative abundances of bacterial families that the sample size of any microbiome study needs to be considered. We therefore suggest that the control sample size of such studies should preferably involve at least 10 animals to account for variability. Evaluation of core bacterial taxa respective to the treatments showed that controls, restricted diet and, to a slightly lesser extent, Streptomycin sulfate treatment groups had high abundances of Firmicutes and Bacteroidetes phyla, which was also observed by Bao et al. in mice [38]. As Streptomycin sulfate is not effective against the majority of the gut microbiota, very similar relative abundances of bacterial families in the treated and control groups can be expected, even in different species. The overall diversity of both the lincosamides looked similar, consistent to what was observed before [15]. Both the lincosamides=treated animal groups showed high abundances of Firmicutes and Proteobacteria, while Bacteroidetes levels were extremely reduced similar to what was seen in Behr et al. [15]. Most anaerobic bacteria that otherwise dominated the gut microbiota of control animals were wiped off by the two lincosamides. Roxithromycin showed the highest levels of Firmicutes and Bacteroidetes, as also shown by Zheng et al. [39]. Sparflosxacin treatments showed maximum abundances of Verrucomicrobia and Firmicutes phyla. Sparfloxacin, similarly to other quinolones and fluoroquinolones, kills bacteria, including Gram-positive and Gram-negative bacteria and other anaerobes; hence, the abundances of dominant species are reduced, whereas bacteria belonging to families *Verrucomicrobiaceae* and *Lactobacillaceae* increased compared to control animals. Finally, Vancomycin treatment groups showed the highest abundances of Verrucomicrobia and Proteobacteria phyla compared to all the other treatment groups, also wiping out the majority of the otherwise dominant bacteria in control animals. This antibiotic showed the maximum activity against the gut microbiota.

Hierarchical clustering analysis based on the gut bacterial compositions showed that controls and restricted diet clustered together close to Streptomycin and most distant to Vancomycin. Vancomycin was observed to have the maximum dysbiosis compared to all the other antibiotic treatments. Both lincosamides clustered together but had minute differences in the abundances of families, e.g., *Enterococcaceae, Bacillaceae, Peptostreptococ-*

caceae, Eubacteriaceae. Roxithromycin and Sparfloxacin treatments clustered together with minor differences in the abundances of *Eubacteriaceae, Rikenellaceae, Clostridiaceae* and some others. Therefore, we observe antibiotic treatment-specific and class-specific gut composition alterations. Differential abundance analysis showed very minute dose-related effects and sex-dependent differences. The differential abundance results were comparable to the relative abundance stacked bar, where dominant/rare treatment-specific bacterial families could be observed, which is consistent with the hierarchical clustering analysis.

4.2. Metabolome Analysis

The dose levels of the antibiotics have been chosen as such as to have a significant influence on the gut microbiome, but not to lead to overt adverse effects in the treated animals. The absence of clinical signs of toxicity, effects on body weights and food consumption for most of the tested antibiotics makes it likely that systemic toxicity will not have played a role in the antibiotic treatments. Lincosamides, Roxithromycin and Sparfloxacin are known to be somewhat bioavailable [16], which could have had an influence on the plasma metabolome. At the very beginning of treatment, it might be possible that some clinical effects were noted for the high dose of clindamycin. However, after the first days of the study, the animals adapted to the treatment, and no more clinical signs were observed. To analyze a possible effect of systemic toxicity of the antibiotics on the plasma metabolome, they were administered at high- and low-dose levels to observe any dose-based response, the assumption being that the low and high dose would result in similar effects on the microbiome—which it did—and that therefore additional high-dose-only-related changes in the plasma metabolome would be indicative for systemic or organ toxicity. The different metabolomes of the antibiotic-treated rats can be found in the Supplementary data (see Tables S2–S15). Plasma metabolome data did not show a profound treatment-based effect in the clustering, suggesting that the majority of the altered metabolites had a microbiome origin.

To understand the influence of restricted diet i.e., compromised nutrition on the metabolomes, PCA analyses were performed. Only the plasma metabolome showed a clear separation between controls and the reduced-diet group. This separation was not observed in the feces and cecum metabolomes and 16S bacterial community profile. This indicates that changes in the plasma metabolome induced by nutrition restrictions did not come from the gut microbial metabolism, but instead the host metabolism. Similar findings have been indicated in Zheng et al., who confirm that host-microbial co-metabolites in plasma were majorly changed due to caloric restrictions in humans [40].

Comparing the clustering of fecal metabolome with 16S microbiome clustering, we observed a similar grouping (refer to Figure 7a and Figure S2), indicating that changes in the microbiome community are well correlated with the fecal metabolome profiles. This allows us to associate the 16S bacterial composition directly with the altered fecal metabolite levels to understand gut bacterial metabolism. Clustering analysis of cecum metabolome showed a bit more extensive antibiotic-treatment-specific clustering, but it was almost similar to the clustering of the fecal metabolome (see Supplementary Figure S4).

The overlaps or differences between the correlation analysis of plasma, feces and cecum metabolome showed that cecum and fecal metabolome are highly correlated in line with the results of [41]. Thus, the feces metabolome is as informative as cecum and is a non-invasive method facilitating easy sampling procedures and longitudinal study designs. Further, when plasma metabolome was compared with feces and cecum metabolomes, almost no overlaps were observed, indicating that many of the fecal metabolites are not readily absorbed from the colon. These observations are in line with previous research [42,43].

We found indole-3-acetic acid to be a key biomarker metabolite (Supplementary Figure S8) [15–17]. This metabolite was observed to be significantly reduced in plasma, feces and cecum metabolomes of antibiotic-treated rats. Indole-3-acetic acid is produced either from bacterial indole production or from dietary tryptophan degradation by intestinal bacterial cells. The reduction of this key metabolite could be explained by a substantial loss

of microorganisms, thereby reducing the ability to degrade tryptophan [15,17], and could potentially serve as a quantitative marker.

4.3. Correlation Analysis

Inter-omic correlation analysis between 16S bacterial families and both plasma and fecal metabolites were performed to elucidate the link between microbiome communities and fecal metabolites. We have approached the microbiome/metabolome correlation analysis from a holistic point of view, demonstrating for most metabolites their correlation direction and strength. For a few selected metabolites, for which sufficient knowledge about their formation is available, we provide a more in-depth analysis. Firmicutes, specifically strains belonging to the Clostridium genus, are mainly known as amino-acid-fermenting bacteria, which is consistent with what we see in our feces microbiome–metabolome correlations.

4.3.1. Feces Metabolome-Microbiome

The majority of amino acids (see Figure 9) are upregulated in treatments that have more than 10-fold reduced *Prevotellaceae* levels in animals treated with lincosamides and Sparfloxacin antibiotics. Fluoroquinolones such as Sparfloxacin and lincosamides including Clindamycin are known to be active against this bacterial family [44,45]. Most gut bacteria are known to use amino acids as a preferred N-source. Arginine-to-ornithine conversion is also well studied in gut bacterial metabolism. In our correlation analysis, we see that levels of arginine are higher in Sparfloxacin treatment groups, and levels of ornithine are even higher in the feces of Sparfloxacin-treated animals. The Sparfloxacin treatment group has the highest abundance of *Peptostreptociccaeae* compared to controls and all the other treatments, which could indicate why the levels of ornithine in the feces of Sparfloxacin treated Wistar rats are significantly higher than in feces of all the others. We observed that amino acids such as glutamine, aspartate, lysine, valine (all branched-chain amino acid), threonine, serine and glycine were all significantly upregulated in all the treatments except for the restricted diet and Streptomycin treatment, indicating that reduced numbers of bacterial taxa are associated with reduced amino acid consumption. An overview of amino acid biosynthesis by gut microflora in humans and animals can be found in Dai et al. [46]. Three bacterial families, *Lactobacillaceae, Verrucomicrobiaceae* and *Anaeroplasmataceae*, form clusters of highly positive correlations with amino acids such as glycine, leucine, isoleucine, phenylalanine, alanine, valine and proline, suggesting common functions between these bacterial families.

Some of the amino acid fermentation products of gut bacteria include indole compounds such as tryptophan and organic acids such as lactate [46]. Tryptophan concentrations in all the treatments except for restricted diet and Streptomycin treatment groups were significantly increased. In particular, both lincosamide treatment groups (Clindamycin and Lincomycin) had very high levels of tryptophan in the feces, indicating that they reduced the bacterial taxa responsible for the conversion of tryptophan to indolic metabolites. It should be noted that *E. coli* strains belonging to the family *Enterobacteriaceae* are involved in the production of bacterial tryptophan and that these may also have been affected [47]. Kynurenic acid that results from tryptophan metabolism was significantly increased in the feces of Roxithromycin-, Streptomycin- and Vancomycin-treated animals. This indicates that the tryptophan was used by bacterial taxa occurring in these treatments. The Clindamycin treatment group had extremely high amounts of tryptophan; we also observed that kynurenic acid levels in the feces of these treatments also significantly increased compared to other treatments, but the levels were lower than tryptophan levels. This shows that there must be bacterial transformation from tryptophan to kynurenic acid occurring in Clindamycin-treated animals, and that tryptophan production is much higher than the bacterial conversion of Tryptophan to Kynurenic acid, as shown by [48]. Glucuronic acid, which is also a product of tryptophan metabolism, was observed to be significantly increased in Sparfloxacin and Vancomycin treatment groups. In our correlation analysis,

glucuronic acid had the strongest positive correlation with *Rikenellaceae*, *Verrucomicrobiaceae* and *Anaeroplasmataceae* families, which are highest in abundance in Sparfloxacin- and Vancomycin-treated animals. This could mean that these families play a specific role in the conversion of tryptophan to glucuronic acid. Pyruvate, an energy-related metabolite was significantly downregulated in the feces of all the treatments, whereas glucose levels were significantly upregulated in all the treatment groups except the restricted diet group, demonstrating that bacterial gluconeogenesis is altered by all the drugs.

A key metabolite of gut microbial metabolism is indole-3-acetic acid (IAA) [17]. The correlation analysis shows few weakly positive and many weakly negative correlations with the majority of bacterial families except *Verrucomicrobiaceae* and *Anaeroplasmataceae*, with strongly negative correlations. IAA levels in feces only significantly increased in Clindamycin treatment groups, whereas they were significantly lowered in all the other treatments. Bacterial IAA is known to be biosynthesized by Gram-negative and Gram-positive bacteria involving decarboxylation and deamination of tryptophan. Tryptophan-dependent pathways for IAA production include either indole-3-pyruvic acid (IPA) and indole-3acetamide (IAM), or indole-3-acetonitrile (IAN) as important intermediates [49]. The fact that tryptophan levels were highly increased in the feces of animals treated with Lincomycin and Sparfloxacin, while IAA levels were significantly reduced, means that the conversion from tryptophan to IAA did not occur in these treatment groups. In the Clindamycin treatment groups, however, both tryptophan and IAA were increased in the feces, suggesting that there must be bacterial transformation directly from indole to IAA occurring in Clindamycin treatments unlike other treatments. Feces from Clindamycin-treated animals were observed to possess *Enterococcaceae* families in the highest abundance compared to all the other treatment groups, so it could be hypothesized that these families are responsible for the production of IAA from indole directly via a tryptophan-independent pathway.

Creatine and creatinine are both utilized by gut microbes for growth. Conversion of creatinine to creatine is not possible by mammalian metabolism, and creatinine is eliminated from the system. While bacteria belonging to Firmicutes and Proteobacteria phyla have been extensively studied to possess creatine degradation activity [48], creatinine levels in the feces were weakly correlated with almost all the bacterial families except *Porphyromonadaceae* and *Prevotellaceae*, which belong to Bacteroidetes phyla. Creatinine levels were highly significantly increased in the feces of all the treatment groups except for restricted diet and Streptomycin treatments, indicating that most of the facultative anaerobes dominating the gut of the animals belonging to these two treatment groups continue to utilize creatinine for further metabolism. Levels of creatine in the feces of lincosamides-and Vancomycin-treated animals are not as high as creatinine, which means there is a conversion of creatinine to creatine occurring in these three treatment groups, but there is also accumulation of creatinine. This means that either there are other bacterial taxa that produce creatinine, or they do not carry out the conversion from creatinine to creatine in an efficient way. Relative abundances of *Porphyromonadaceae* and *Prevotellaceae* families are highest in restricted diet and Streptomycin treatment groups, where creatinine levels are not altered in the feces, suggesting that they may play a role in creatine metabolism. Metabolites that result from microbiome-mediated metabolism include lipids and lipoproteins, amino acids, glutamate, choline, acetate, butyrate and glycerol [50]. We also see similar results in our correlations analysis where bacterial taxa produced the strongest correlations with metabolites belonging to amino acids, lipids and fatty acids derivate classes in the feces. Clusters of positive correlations between specific bacterial families including *Porphyromonadaceae, Ruminococcaceae, Lachnospiraceae, Bacteroidaceae, Prevotellaceae, Bdellovibrionaceae* and *Peptococcaceae* could be observed with metabolites belonging to lipids, fatty acids and related classes, suggesting common functions between these bacterial families. All in all, the correlations showed most of the strongly correlated metabolites belonging to amino acids, lipids and related metabolites, in line with [51,52]. Our results on the role of gut bacteria in amino acid, complex lipids and fatty acid synthesis are similar to those published by Fujisaka et al. [43].

4.3.2. Plasma Metabolome-Microbiome

Although tryptophan levels in plasma were not altered significantly in any of the treatment groups, glucuronic acid resulting from tryptophan metabolism is significantly upregulated in most of the treatment groups, except the restricted diet, Vancomycin and Streptomycin treatment groups. In the correlation analysis, plasma tryptophan and glucuronic acid do not show any strong correlation with the gut bacterial families. This could mean that these metabolites could be from dietary sources and a result of host metabolism. Plasma creatine and creatinine clustered together in the correlation heatmap. Creatinine levels in all the treatment groups did not show a large alteration, but creatine showed significant downregulation only in the restricted diet group. As restricted-diet-fed animals did not have a large influence on the gut microbial dysbiosis, it could be concluded that this increase in creatine levels in plasma is related to host metabolism. The gut microbiome is extensively known to metabolize dietary tryptophan into indole, and its derivatives, such as indole-3-acetic acid (IAA) and indole-3-propionic acid (IPA)m which are also absorbed efficiently by the gut mucosa [53]. Plasma IAA was observed to be highly upregulated in the plasma of Vancomycin-treated animals. The *Verrucomicrobiaceae* family is highly abundant in this treatment group. This could potentially mean the higher abundance of this bacterial family contributed in the production of IAA, thereby increasing the levels, which is also described in Louis et al., where they identify specific colonic bacteria including Verrucomicrobia phyla that contribute to the production of propionate and butyrate in humans [54].

3-Indoxylsulfate (IS) in plasms was downregulated in the two lincosamides treatment groups and highly upregulated in the Roxithromycin treatment group. This could mean that in Roxithromycin treatment, the bacterial production of IS was higher due to the higher abundance of bacterial taxa such as *Eubacteriaceae*, which supports this conversion [55]. Tryptophanase activity of the gut bacteria is known to convert tryptophan to indole, which further gets absorbed in the gut and transformed to IS in the liver, which leads to an increase in plasma IS levels [56]. Overall, the 16S bacterial families were associated more with plasma metabolites belonging to amino acid classes, but also carbohydrates, energy metabolites and lipids, nucleic acids and related metabolites, which is consistent with what is observed in Fujisaka et al. [43]. 16S bacterial families showed high numbers of strong correlations (irrespective of the direction) with feces and cecum metabolites, whereas very limited correlations could be observed with plasma metabolites (see Figure 11).

4.4. Bile Acids

We conducted an extensive analysis for individual antibiotics on their influences on bile acid levels and tried to associate them with the responsible bacterial families. A standard workflow including the majority of the bile acid reactions combined is shown in Figure 13, where we can see which bile acids are produced in the liver and which ones are produced by the gut bacteria.
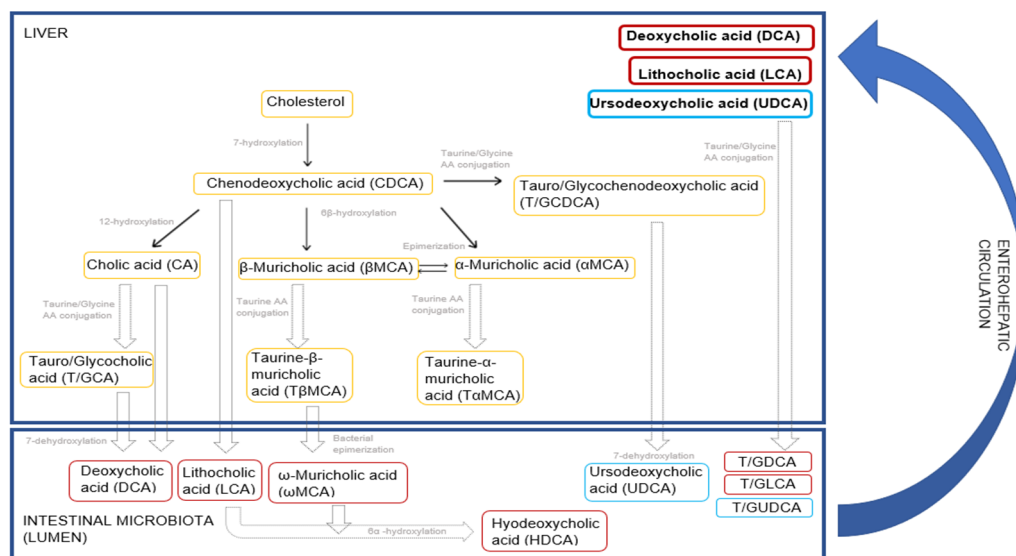
Figure 13. Host and gut microbiota-mediated bile acid metabolism in rodents. The schematic diagram shows yellow boxes for bile acids that are primarily synthesized in the liver, red boxes for secondary bile acids that are biotransformed from the primary bile acids by the gut microbiota and blue boxes for the tertiary bile acid that enters the enterohepatic circulation. Primary, secondary and tertiary bile acids are reabsorbed from the GI walls and re-enter the liver via enterohepatic circulation to stabilize the bile acid pool. This figure was made based on previous publications [57,58].

4.4.1. Clindamycin Hydrochloride Treatment

CDCA is the first metabolite that is produced from CYP enzyme-mediated hydroxylation activity of cholesterol in the liver. Following treatment with Clindamycin, CDCA levels are observed to be significantly downregulated in plasma and feces. This could mean an increased conversion of CDCA to its conjugated forms or a reduced production due to reduced 7-hydroxylation activity. Conjugated primary bile acids such as TCDCA and GCDCA are formed from CDCA as a precursor. Rodents are known to preferentially conjugate in the liver using taurine (almost 90%) rather than Glycine [52], and our findings are in line with this knowledge. CA is formed from further hydroxylation of CDCA in the liver. CA levels were significantly upregulated in feces but downregulated in plasma. This could mean either that its precursor CDCA levels are reduced in plasma (as observed in Table 2) and hence that there is a significant downregulation of CA in plasma, or that CA could not be converted to DCA by the gut bacterial enzymes due to lack of gut microflora bioactivity. These two hypotheses are in line with our data that both CDCA and DCA levels were indeed reduced. This is also consistent with what we see in our data as TCDCA is highly upregulated in the feces compared to GCDCA, as would be expected from the preferential conjugation with taurine amino acids in rats. This also means that TCDCA is not deconjugated in the gut. Despite the profound increase in conjugated bile acids in the feces, in plasma, TCDCA levels are only marginally upregulated, whereas GCDCA are significantly downregulated. Consequently, reabsorption of both conjugated bile acids would appear to be very limited. Two of the other primary bile acids that result from hydroxylation of CDCA are MCA alpha and MCA beta. The feces and plasma levels of MCA (both alpha and beta) are significantly downregulated. The suggested hypothesis is that the conjugation step from MCA (alpha and beta) to taurine-conjugated TMCA (alpha and beta) must be higher in the clindamycin treatment group. This is very much in line with what we observe, as the TMCA (both alpha and beta) levels are highly significantly increased in feces, whereas in the plasma, the TMCA (alpha and beta) levels are only weakly upregulated. Taurine conjugate bile acids are known to be absorbed in the gut, providing an explanation for the increased levels of TMCA in plasma. Other taurine- and glycine-conjugated bile acids that are produced from CA are TCA and GCA. GCA is observed to be downregulated in both plasma and feces, whereas TCA is observed to be

highly significantly upregulated in feces and downregulated in plasma. Upregulation of TCA in feces could correspond to more rapid conjugation of CA to TCA than to GCA and weak reabsorption of them from the small intestine.

Table 2. Fold changes of different bile acid levels going up (red boxes) and down (blue colored boxes) in the feces and plasma matrices of male and female Wistar rats of Clindamycin treatment (*p*-value depends on the shade of the colors, the darkest red is *p*-value < 0.01, medium red is *p*-value < 0.05; and the lightest shade of red is *p*-value < 0.10 and similarly for blue coloring). F represents females, M represents males, 7 d, 14 d and 28 d denote blood sampling time points days 7, 14 and 28, respectively.

Metabolite Name	Analyte Name	Feces		Plasma					
		F	M	F 7d	F 14d	F 28d	M 7d	M 14d	M 28d
Cholate	CA	18.64	19.90	0.02	0.03	0.01	0.01	0.03	0.01
Chenodeoxycholate (chenodeoxycholic acid)	CDCA	0.30	0.08	0.02	0.03	0.04	0.02	0.10	0.02
Deoxycholate (deoxycholic acid)	DCA	0.00	0.00	0.35	0.00	0.01	0.10	0.36	0.01
Glycocholate, glycocholic acid	GCA	1.72	0.47	0.44	0.30	0.21	0.22	0.35	0.16
Glycochenodeoxycholate (glycochenodeoxy-cholic acid)	GCDCA	2.67	0.09	0.56	0.40	0.76	0.06	0.08	0.06
Glycodeoxycholate, -cholic acid	GDCA	0.58		0.04		0.07	0.01	0.01	0.02
Glycolithocholic aicd	GLCA	0.52	0.44	0.54	0.26	0.68	0.12	0.79	0.36
Glycoursodeoxycholic acid	GUDCA	2.82	2.25	0.11	1.03			0.97	0.30
Hyodeoxycholate, hyodeoxycholic acid	HDCA	0.00	0.00	0.01	0.01		0.00	0.01	0.00
Lithocholate, lithocholic acid	LCA	0.01	0.01	1.00			0.53	1.55	0.35
Muricholic acid (alpha)	MCAa	0.59	0.16	0.03	0.06	0.06	0.01	0.02	0.01
Muricholic acid (beta)	MCAb	2.36	0.87	0.11	0.25	0.39	0.15	0.31	0.39
Muricholic acid (omega)	MCAo	0.06	0.01	0.00	0.01	0.04	0.01	0.00	0.01
Taurocholate, taurocholic acid	TCA	47.42	90.80	1.34	1.01	1.63	4.68	2.94	4.56
Taurochenodeoxycholate	TCDCA	35.03	13.64	1.38	0.99	1.54	2.46	1.46	1.25
Taurodeoxycholate, -cholic acid	TDCA	0.25	0.15	0.02	0.01	0.01	0.01	0.01	0.05
Taurolithocholic aicd	TLCA	0.15	0.34	0.04		0.04	0.19	0.14	0.19
Tauromuricholic acid (a + b)	TMCA (a + b)	155.83	192.72	1.96	1.41	2.38	4.97	2.57	3.99
Tauroursodeoxycholic acid	TUDCA	22.61	28.27	6.92			0.20	0.57	0.74
Ursodeoxycholate, Ursodeoxycholic acid, Ursodiol	UDCA	0.02	0.03	0.05	0.27	0.01	0.01	0.30	0.02

The most enigmatic data are the profound upregulation of CA in the feces and similarly profound downregulation in the plasma. This would strongly suggest that there is a lack of resorption of CA in the lower intestinal tract and in fact a loss of CA to the entire biological system.

Taurine-conjugated CA was reabsorbed; hence, we see an upregulation in the plasma. Secondary bile acids that result from bacterial deconjugation are namely DCA, LCA, MCAo

and HDCA. In our data DCA, MCAo and HDCA levels show significant downregulation in both plasma and feces, again demonstrating impairment of bacterial deconjugation reactions. This is also in line with their precursor bile acids TCA and TMCA (both alpha and beta) levels being significantly upregulated in the feces. The tertiary bile acid UDCA produced from the downregulated secondary bile acid LCA is also reduced in both feces and plasma of this treatment group. The literature indicates that UDCA is produced from LCA in the intestine [59] or in the liver [60]. In our study, we see LCA levels reduced in the feces but unaffected in the plasma. Therefore, it would seem more likely that UDCA is produced in the gut rather than the liver. This could be because this metabolite gets reabsorbed into the liver and gets readily conjugated into its taurine form. This is in line with the TUDCA levels highly significantly upregulated in the feces. This proves the increased conjugation of the tertiary bile acid and lack of deconjugation in the gut. Other deconjugated secondary bile acids such as DCA and LCA can also be reabsorbed and enter into the liver for the conjugation reaction. Due to the impairment in the production of these secondary bile acids by the disturbed gut bacteria, the taurine/glycine-conjugated DCA and LCA also appear to be significantly downregulated in both plasma and feces. Taurine deconjugation is less likely to have happened according to our data. Glycine-conjugated bile acids look far less affected. This proves that Clindamycin-treated rats have overall impaired secondary bile acid production which is exactly what we expect after treating the animals with an antibiotic.

As Clindamycin is a member of the lincosamide group, it is no surprise that Lincomycin has a similar anti-biotic spectrum. Lincomycin-treated animals also show a clear impairment of secondary bile acid production due to perturbations in the gut flora. Both the antibiotics belong to the same class of antibiotics called Lincosamides, and they definitely show a similar influence on the bile acid profiles. The table of altered bile acid metabolites in the plasma and feces of lincomycin hydrochloride treatment group can be seen in the supplementary data (see Table S17). This altered bile acid levels in the feces and plasma of the two lincosamide treatment groups could be associated with the extreme downregulation of Firmicutes (including bacterial families such as *Lachnospiraceae*, *Peptpcoccaceae* and *Petptostreptococcaceae*), Bacteroidetes (including bacterial families such as *Prevotellaceae*, *Bacteroidaceae* and *Porphyromonadaceae*) and Proteobacteria (including bacterial families such as *Bdellovibrionaceae*, *Rhodospirillaceae*, *Desulfovibrionaceae*) compared to the control animals (see DESeq2 Table S16). The reduction in levels of these previously mentioned bacteria may be related to the impairment of secondary bile acid production in those treatment groups.

4.4.2. Vancomycin Treatment

CDCA levels in the feces of Vancomycin treatment group do not appear to be significantly altered, whereas in the plasma, we observe a consistent downregulation of CDCA, as shown in Table 3. As we do not see a significant change in CDCA levels in the feces, it can be expected that metabolites such as TCDCA, GCDCA and MCA (both alpha and beta) should not be changed in the feces of this treatment group either. This is in line with what we see in our data. GCDCA, TCDCA and MCA (both alpha and beta) do not show significant changes in the feces of vancomycin-treated animals.

Table 3. Fold changes of different bile acid levels going up (red cooled boxes) and down (blue boxes) in the feces and plasma matrices of male and female Wistar rats of Vancomycin treatment (*p*-value depends on the shade of the colors; the darkest red represents *p*-value < 0.01, medium red represents *p*-value < 0.05 and the lightest shade of red represents *p*-value < 0.10, and similarly for blue). F represents females, M represents males, 7 d, 14 d and 28 d denote blood sampling time points days 7, 14 and 28, respectively.

Metabolite Name	Analyte Name	Feces		Plasma					
		F	M	F 7d	F 14d	F 28d	M 7d	M 14d	M 28d
Cholate	CA	19.45	38.66	0.18	0.60	0.14	0.10	0.13	0.13
Chenodeoxycholate (chenodeoxycholic acid)	CDCA	4.30	0.99	0.18	0.36	0.05	0.10	0.16	0.18
Deoxycholate (deoxycholic acid)	DCA	0.00	0.00	0.01	0.42	0.01	0.00	0.18	0.00
Glycocholate, glycocholic acid	GCA	2.67	1.45	0.46	1.54	0.73	0.39	0.36	0.18
Glycochenodeoxycholate (glycochenodeoxy-cholic acid)	GCDCA	1.01	1.54	0.39	0.87	0.64	0.30	0.27	0.42
Glycodeoxycholate, -cholic acid	GDCA	0.32	0.34	0.02	0.07	0.03	0.01	0.00	0.05
Glycolithocholic aicd	GLCA	0.24	0.86	0.56	0.21	0.20	0.48	1.65	4.39
Glycoursodeoxycholic acid	GUDCA	1.44	1.44	1.65	1.18	3.31	0.43	16.34	10.13
Hyodeoxycholate, hyodeoxycholic acid	HDCA	0.00	0.00	0.01	0.01	0.00	0.00	0.00	0.00
Lithocholate, lithocholic acid	LCA	0.01	0.07	0.12	10.74	0.15	0.35	27.95	0.19
Muricholic acid (alpha)	MCAa	0.44	0.71	0.21	0.44	0.10	0.13	0.14	0.23
Muricholic acid (beta)	MCAb	0.50	0.53	0.54	1.01	1.35	0.17	0.18	0.38
Muricholic acid (omega)	MCAo	0.02	0.03	0.05	0.01	0.07	0.03	0.01	0.02
Taurocholate, taurocholic acid	TCA	4.18	7.39	2.04	6.99	3.83	2.47	2.71	2.62
Taurochenodeoxycholate	TCDCA	0.99	3.04	1.87	2.42	2.64	2.69	3.18	2.97
Taurodeoxycholate, -cholic acid	TDCA	0.16	0.09	0.01	0.02	0.01	0.01	0.01	0.01
Taurolithocholic aicd	TLCA	0.42		0.03	0.04	0.03	0.12	0.18	1.58
Tauromuricholic acid (a + b)	TMCA (a + b)	2.86	3.89	3.10	4.02	3.59	1.93	2.71	3.11
Tauroursodeoxycholic acid	TUDCA	0.54	2.93	3.61	1.82		1.23		0.79
Ursodeoxycholate, Ursodeoxycholic acid, Ursodiol	UDCA			0.21	0.06	0.29	0.13	0.12	0.23

As with the lincosamide antibiotics, for Vancomycin, we also noted a profound increase in CA in the feces and a downregulation in the plasma, indicating that CA is not well resorbed from the lower intestinal tract. As DCA levels were very much reduced in the feces, this means that 7-alpha-dehydroxylation of CA was severely impaired, due to the change in the microbiome composition. We saw significant downregulation of DCA, a secondary bile acid, in both plasma and feces, again indicating impairment of bacterial deconjugation from TCA or GCA to DCA. Therefore, TCA as the preferred conjugated of CA was highly upregulated in both plasma and feces. Taurine-conjugated primary bile acids, including TCA, TMCA alpha and beta, are also highly upregulated in both

plasma and feces, again in line with the lack of microbial deconjugation. As a consequence, secondary bile acids like DCA, LCA, MCAo and HDCA are downregulated in both plasma and feces. These secondary bile acids, including tertiary bile acid UDCA, can be reabsorbed in the gut and become reconjugated with Taurine or Glycine AA. However, as their levels are reduced, the levels of G/TDCA and G/TLCA are also significantly downregulated in both plasma and feces. Taking into account the microbiome changes induced by Vancomycin, this could be related to the downregulation of many Bacteroidetes and Firmicutes phyla. Qualitatively, the overall changes in the bile acid levels induced by these antibiotics (vancomycin and lincosamides) are similar, but quantitatively, we see marginal differences.

4.4.3. Sparfloxacin Treatment

Many of the changes in BAs seen following Sparfloxacin-treated animals were similar to the ones described for the lincosamides and vancomycin groups (see Table 4). Again, profound changes were noted for CA in feces, DCA in feces and plasma and upregulation of particularly taurine-conjugated BAs in both feces and plasma.

Table 4. Fold changes of different bile acid levels going up (red boxes) and down (blue colored boxes) in the feces and plasma matrices of male and female Wistar rats of Sparfloxacin treatment (*p*-value depends on the shade of the colors; the darkest red represents *p*-value < 0.01, medium red represents *p*-value < 0.05 and the lightest shade of red represents *p*-value < 0.10, and similarly for blue). F represents females, M represents males, 7 d, 14 d and 28 d denote blood sampling time points days 7, 14 and 28, respectively.

Metabolite Name	Analyte Name	Feces		Plasma					
		F	M	F 7d	F 14d	F 28d	M 7d	M 14d	M 28d
Cholate	CA	27.39	22.73	1.08	0.46	0.32	0.11	0.91	0.90
Chenodeoxycholate (chenodeoxycholic acid)	CDCA	0.52		0.32	0.17	0.37	0.04	0.28	0.94
Deoxycholate (deoxycholic acid)	DCA	0.01	0.00	0.09	0.02	0.08	0.01	0.18	0.03
Glycocholate, glycocholic acid	GCA	1.88	1.57	1.02	0.53	2.05	0.42	0.59	0.71
Glycochenodeoxycholate (glycochenodeoxycholic acid)	GCDCA	1.25	2.93	0.51	0.34	1.61	0.14	0.13	0.40
Glycodeoxycholate, -cholic acid	GDCA		2.70	0.08	0.25	0.51	0.02	0.01	0.12
Glycolithocholic aicd	GLCA	8.22	1.33		0.90	0.71	0.24		1.93
Glycoursodeoxycholic acid	GUDCA	0.96	1.61					0.33	1.30
Hyodeoxycholate, hyodeoxycholic acid	HDCA	0.01	0.00	0.06	0.01		0.00	0.00	
Lithocholate, lithocholic acid	LCA	0.24	0.01	0.12	0.01	13.09	0.18	9.66	0.31
Muricholic acid (alpha)	MCAa	0.58	0.16	0.67	0.24	0.57	0.05	0.38	0.73
Muricholic acid (beta)	MCAb	0.33	0.37	1.46	1.21	0.31	0.25	1.87	1.10
Muricholic acid (omega)	MCAo	0.01	0.02	0.20	0.01	0.01	0.01	0.00	
Taurocholate, taurocholic acid	TCA	4.95	8.29	2.61	3.25	1.73	7.96	5.32	3.09
Taurochenodeoxycholate	TCDCA	2.29	4.99	1.21	1.44	1.77	3.85	3.63	2.08
Taurodeoxycholate, -cholic acid	TDCA	0.30	0.18	0.09	0.21	0.03	0.11	0.03	0.04
Taurolithocholic aicd	TLCA	0.27	0.75		1.11	0.06	0.28	0.33	0.22

Table 4. *Cont.*

Metabolite Name	Analyte Name	Feces			Plasma				
		F	M	F 7d	F 14d	F 28d	M 7d	M 14d	M 28d
Tauromuricholic acid (a + b)	TMCA (a + b)	7.08	16.86	1.72	1.73	1.88	4.25	4.95	2.27
Tauroursodeoxycholic acid	TUDCA	2.12	9.35		10.27			7.76	1.82
Ursodeoxycholate, Ursodeoxycholic acid, Ursodiol	UDCA	0.25	0.01	0.36	0.56	0.23	0.13	1.20	1.17

The upregulation of CA in the feces, similar to the lincosamides and vancomycin, could be explained by a negative feedback mechanism associated with the high levels of conjugated bile acids, as a result of the reduced deconjugation steps. As indicated earlier, the reduction of CA in the plasma can be explained by a lack of reabsorption from the colon. GCDCA does not show any significant change in its levels in feces, although it is downregulated in plasma; TCDCA, on the other hand, is highly upregulated in both plasma and feces. This indicates a higher production of TCDCA than GCDCA, as also observed for the other antibiotic treatments; it also indicates that, due to interrupted bacterial deconjugation activity, these get accumulated in the feces. The Taurine-conjugated bile acids are reabsorbed from the gut and their elevated levels also result in increased plasma levels. MCA (both alpha and beta) show major downregulation in both plasma and feces, indicating that they are readily converted to their conjugated forms. The Taurine conjugate of MCA both alpha and beta (TMCA a+b) show high upregulation in both plasma and feces, confirming that the Taurine conjugation of MCA, both alpha and beta, is high in Sparfloxacin treatment groups. Secondary bile acids, including DCA, LCA, MCAo and HDCA, all show downregulation in both plasma and feces, indicating impairment in deconjugation by bacterial enzymes, thereby reducing their levels in both plasma and feces, which is consistent with UDCA a tertiary BA. In our data, G/TDCA, G/TLA and GUDCA show no change in their levels in both plasma and feces, whereas TUDCA shows upregulation in both plasma and feces, indicating that whatever UDCA levels were sent to the liver were then readily reconjugated with Taurine, after which further deconjugation by the gut bacteria did not occur, leading to high levels in the feces. This is very similar to the lincosamide treatment group and can be linked to downregulation of Proteobacteria and Firmicutes phyla compared to controls.

4.4.4. Roxithromycin Treatment

This roxithromycin treatment group showed very interesting results compared to all the antibiotics (see Table 5). CDCA levels in the plasma of the roxithromycin treatment group showed significant downregulation, whereas no significant changes in the feces were observed. This is consistent with what was observed in the other antibiotic treatment groups. CA is significantly downregulated in feces, an effect not observed in any of the other antibiotic treatment groups. Comparing this observation with the microbiome composition following roxithromycin treatment, it is noted that there is a unique upregulation of the *Rikenellaceae* in this group.

Table 5. Fold changes of different bile acid levels going up (red boxes) and down (blue colored boxes) in the feces and plasma matrices of male and female Wistar rats of Roxithromycin treatment (*p*-value depends on the shade of the colors; the darkest red is *p*-value < 0.01, medium red is *p*-value < 0.05 and the lightest shade of red is *p*-value < 0.10, and similarly for blue). F represents females, M represents males, 7 d, 14 d and 28 d denote blood sampling time points days 7, 14 and 28, respectively.

Metabolite Name	Analyte Name	Feces		Plasma					
		F	M	F 7d	F 14 d	F 28 d	M 7 d	M 14 d	M 28 d
Cholate	CA	0.52	0.55	0.04	0.05	0.13	0.00	0.00	0.02
Chenodeoxycholate (chenodeoxycholic acid)	CDCA	0.90		0.02	0.06	0.08	0.02	0.01	0.05
Deoxycholate (deoxycholic acid)	DCA	0.49	0.70	0.75	0.58	0.86	0.15	0.11	0.20
Glycocholate, glycocholic acid	GCA	0.15	0.23	0.42	0.30	0.10	0.25	0.10	0.08
Glycochenodeoxycholate (glycochenodeoxy-cholic acid)	GCDCA	0.42	0.72	0.39	0.36	0.17	0.38	0.10	0.08
Glycodeoxycholate, -cholic acid	GDCA		0.49	0.51	0.37	0.07	0.14	0.05	0.07
Glycolithocholic aicd	GLCA	0.41	1.63	0.28	0.27	0.49	0.33	0.93	0.66
Glycoursodeoxycholic acid	GUDCA	1.44		1.82	0.59	1.13	0.46	1.45	0.63
Hyodeoxycholate, hyodeoxycholic acid	HDCA	0.06	0.03	0.10	0.04	0.10	0.01	0.01	0.01
Lithocholate, lithocholic acid	LCA	0.23	0.35	0.71	0.46	0.72	0.64	6.52	0.50
Muricholic acid (alpha)	MCAa	0.73	0.62	0.22	0.19	0.11	0.08	0.02	0.05
Muricholic acid (beta)	MCAb	1.33	0.84	0.71	1.30	2.28	0.16	0.05	0.22
Muricholic acid (omega)	MCAo	0.77	0.60	1.19	0.60	1.47	0.74	0.36	0.42
Taurocholate, taurocholic acid	TCA	2.41	1.58	2.59	5.55	3.14	3.35	2.19	3.77
Taurochenodeoxycholate	TCDCA	1.42	1.54	1.69	1.48	1.84	2.07	2.02	2.28
Taurodeoxycholate, -cholic acid	TDCA	9.42	4.61	2.29	3.11	1.89	2.55	1.19	2.06
Taurolithocholic aicd	TLCA	3.26	3.13	0.74	0.75	1.39	1.05	0.68	0.61
Tauromuricholic acid (a + b)	TMCA (a + b)	10.14	7.97	1.94	2.94	2.37	3.62	2.67	3.02
Tauroursodeoxycholic acid	TUDCA	3.42	2.20	9.03	1.23		1.24		0.55
Ursodeoxycholate, Ursodeoxycholic acid, Ursodiol	UDCA			0.11	0.06	0.53	0.03	0.05	0.01

The reduction of CA levels is in line with the reduced CDCA levels in plasma; however, as the precursor cholesterol was not affected (data not shown), a hypothesis could be that there is increased conjugation of CDCA. This is not at variance with the increased TCDCA levels in the plasma.

Other conjugated bile acids of CDCA, namely GCDCA and TCDCA, showed contrasting levels in plasma and feces. GCDCA was not significantly altered in feces but was downregulated in plasma, and TCDCA levels were highly upregulated in both plasma and feces. This again proves that taurine conjugation is higher than glycine conjugation and that taurine-conjugated BAs are readily reabsorbed in the gut. MCA, both alpha

and beta, showed no alteration in the feces but downregulation in the plasma matrix of Roxithromycin antibiotic treatment group. This indicates that the hydroxylation reaction from CDCA to MCA alpha and beta and further conjugation of MCA alpha and beta to TMCA alpha and beta must be regulated in a way that it does not alter the levels of MCA alpha and beta. TMA alpha and beta are highly upregulated in both plasma and feces, indicating no further deconjugation of these metabolites, leading to an increase in their levels. Secondary bile acids such as LCA, DCA and HDCA were downregulated in both plasma and feces, showing the impairment in bacterial deconjugation in the gut due to antibiotic treatment. MCAo, on the other hand, which is also a secondary BA, did not show a significant change in feces and plasma. These secondary bile acids were reabsorbed from the gut, entered the enterohepatic circulation and were reconjugated with taurine or glycine. Glycine conjugated secondary BA, including GDCA, GLCA and GUDCA, showed significant downregulation in both plasma and feces, indicating a lack of deconjugation and impairment in their levels in the gut before being reconjugated in the liver. In contrast, taurine-conjugated secondary and tertiary BA, including TDCA, TLCA and TUDCA, showed an upregulation in feces and plasma of the Roxithromycin treatment group. Upregulation of TDCA and TLCA in the feces and plasma has not been observed in any of the other antibiotic groups. Taurine conjugation of primary as well as secondary BAs was increased by this antibiotic. This increased taurine conjugation could also be related to an altered FXR signaling pathway. Three BAs including CDCA, DCA and LCA reduce the 7-hydroxylase activity as a negative feedback via the FXR receptor. Even though CDCA, DCA and LCA were significantly low in both plasma and feces of antibiotic treatment groups, in this case, the 7-hydroxylase activity cannot be high. This would indicate that there were more factors playing a role in the maintenance of BA pool, and as we obviously disturbed them using antibiotics, these factors should be microbiome-derived. This could mean that further deconjugation of these taurine-conjugated secondary BAs are impaired, leading to an increase in their levels in feces and plasma.

Two major conclusions that can be derived analyzing the bile acid profiles of Roxithromycin treated animals are that, firstly, 7α dehydroxylase activity of the gut bacterial species present in this treatment group must be high because CA levels are reduced in the feces and are metabolized to secondary bile acids. This could be associated with the highest abundances of *Rikenellaceae* family in this antibiotic treatment compared to controls and other treatments. Hence, these families of bacteria may be the primary source of 7α dehydroxylase activity, which is otherwise absent in the other antibiotic treatment groups. Secondly, we can assume that the taurine deconjugation is still impaired in this treatment group due to the higher accumulation of taurine-conjugated primary and secondary bile acids in both plasma and feces. This could be explained by the reduced abundances of bacterial families such as *Bacteroidaceae, Porphyromonadaceae* and *Prevotellaceae* in this antibiotic treatment, which might be responsible for the taurine amino acid deconjugation in the gut. Cholesterol levels in feces do not change significantly, meaning that bile acids somehow maintain the pool in such a way that the source cholesterol levels are not altered much.

4.4.5. Streptomycin Sulfate Treatment

Amongst all the other antibiotics, this treatment showed the least significantly altered bile acid levels, as shown in Table 6. CDCA levels are only marginally altered in both plasma and feces; hence, we only see marginal effects in GCDCA and TCDCA levels. This nevertheless shows very consistent increases in CA levels in feces and decreases in plasma, which is consistent with the other antibiotic treatments except Roxithromycin. Taurine and Glycine conjugates of CA, namely TCA and GCA, did not show a profound alteration in feces. This is unique amongst all of the antibiotic treatment groups. We note a moderate increase of TCA in the plasma, however. Overall, this suggests that deconjugation reactions are far less impaired by Streptomycin treatment. As this antibiotic causes only relatively moderate changes in the lower intestinal tract microbiome, it can be concluded that deconjugation reactions are occurring at this site. Moreover, further Streptomycin-

specific changes have been observed in MCA alpha and beta levels. Unlike all the other antibiotics, these bile acids are significantly upregulated in both plasma and feces. We also see an upregulation in both alpha and beta TMCA levels in both plasma and feces. We can deduce that Streptomycin has a specific influence on hydroxylation of CDCA to produce MCA alpha and beta, because of which their levels are unusually increasing compared to all the other antibiotic treatments. Secondary bile acid DCA shows very marginal alteration, indicating that their production or bacterial deconjugation is not profoundly disturbed in the case of this antibiotic treatment group. However, other secondary bile acids such as LCA and HDCA show significant downregulation in both plasma and feces, indicating that this part of the bacterial transformation is impaired in Streptomycin, which is consistent with all other antibiotics. On the contrary, we see an upregulation in MCA-omega in both plasma and feces, which is again Streptomycin-specific. This indicates that Muricholic acid and related conjugates and deconjugated metabolites are altered by this antibiotic. We also see MCAo being reabsorbed in this antibiotic treatment, which was not observed in any of the other treatment groups. Taurine-conjugated secondary bile acids were not altered that much, but Glycine-conjugated ones were significantly downregulated. In these treatment groups, Taurine conjugation of reabsorbed secondary bile acids did not show a prominent influence whereas, a downregulation in Glycine conjugated secondary bile acids have been observed in both feces and plasma, which is consistent with what we have observed in other antibiotic treatments.

Table 6. Fold changes of different bile acid levels going up (red boxes) and down (blue boxes) in the feces and plasma matrices of male and female Wistar rats of Streptomycin sulfate treatment (*p*-value depends on the shade of the colors, the darkest red is *p*-value < 0.01, medium red is *p* value < 0.05 and the lightest shade of red is *p*-value < 0.10, and similarly for blue). F represents females, M represents males, 7 d, 14 d and 28 d denote blood sampling time points days 7, 14 and 28, respectively.

Metabolite Name	Analyte Name	Feces				Plasma			
		F	M	F	M	F	M	F	M
Cholate	CA	8.33	3.68	0.49	0.97	0.14	0.71	0.01	0.24
Chenodeoxycholate (chenodeoxycholic acid)	CDCA	17.60	0.56	0.43	1.65	0.17	0.64	0.02	0.37
Deoxycholate (deoxycholic acid)	DCA	1.15	1.56	0.67	0.68	1.22	0.62	0.15	0.31
Glycocholate, glycocholic acid	GCA	1.14	0.29	3.56	0.72	0.58	1.53	0.35	0.26
Glycochenodeoxycholate (glycochenodeoxycholic acid)	GCDCA	0.61	0.70	1.28	0.93	0.98	0.41	0.10	0.31
Glycodeoxycholate, -cholic acid	GDCA	0.39	0.21	1.54	1.02	0.49	0.23	0.05	0.10
Glycolithocholic aicd	GLCA	0.35	1.41	0.46	0.27	0.23	0.39	0.25	0.80
Glycoursodeoxycholic acid	GUDCA	0.89	0.50	1.65	0.61	1.00	1.06	1.24	0.89
Hyodeoxycholate, hyodeoxycholic acid	HDCA	0.20	0.04	0.18	0.25	0.34	0.03	0.01	0.03
Lithocholate, lithocholic acid	LCA	0.35	0.89	0.68	0.39	0.67	0.69	0.35	0.43
Muricholic acid (alpha)	MCAa	2.95	2.43	0.45	1.03	0.42	1.11	0.04	0.32
Muricholic acid (beta)	MCAb	1.07	2.79	1.89	1.81	0.77	1.89	0.53	0.87
Muricholic acid (omega)	MCAo	2.11	1.77	2.17	1.46	2.51	3.19	0.36	0.78
Taurocholate, taurocholic acid	TCA	2.07	1.13	1.73	2.97	2.05	4.50	3.28	2.67
Taurochenodeoxycholate	TCDCA	1.17	1.15	1.22	1.35	2.61	2.54	2.33	2.72

Table 6. *Cont.*

Metabolite Name	Analyte Name	Feces				Plasma			
		F	M	F	M	F	M	F	M
taurodeoxycholate, -cholic acid	TDCA	2.25	0.62	1.66	1.62	2.13	1.68	1.38	1.48
Taurolithocholic aicd	TLCA	0.60	1.68	1.11	0.83	1.05	0.66	0.38	0.47
Tauromuricholic acid (a + b)	TMCA (a + b)	1.86	1.79	1.60	2.44	2.59	3.01	2.64	2.64
Tauroursodeoxycholic acid	TUDCA	1.79	1.04	2.83			1.98		0.63
ursodeoxycholate, ursodeoxycholic acid, ursodiol	UDCA			1.65	0.16	0.20	1.60	0.17	0.39

5. Conclusions

The purpose of the study was to investigate if there are correlations between the microbiome, the fecal metabolome and the host's plasma metabolome. We have clearly demonstrated (1) a close connection between the microbiome and the fecal metabolome. We also noted that (2) the correlation between the fecal and plasma metabolome is much weaker. Moreover, (3) the best correlations between microbiome, fecal and plasma metabolome were obtained for bile acids. In addition, this study provides an extensive set of data for various antibiotic treatments on the gut microbiome and the fecal metabolome. However, the number of all possible combinations (the total of variables) between the microbiome and the metabolome by far exceeds the number of experiments with antibiotics. Therefore, in most cases, a perfect resolution (bacterial species to fecal metabolites) of these observed correlations is not (yet) possible. Overall, we see a huge impact of antibiotic treatments on bacterial deconjugation from primary to secondary and tertiary BA in both plasma and feces. Taurine conjugation is, relative to glycine conjugation, the preferred pathway in all antibiotic treatment groups. Taurine-conjugated primary BAs were readily reabsorbed in the gut and show elevated levels in the plasma. CA levels in the feces were profoundly increased in all treatment groups, except for Roxithromycin, and reduced in the plasma. This is considered to be related to the loss of 7α dehydroxylase activity and the lack of reabsorption of CA from the lower intestinal track. The reduced levels of CA in the Roxithromycin group are correlated with a unique increase of the *Rikenellaceae* family. All antibiotics resulted in increased levels of conjugated bile acids, indicating that they inhibit deconjugation reactions. Streptomycin, which induces the least feces microbiome/caecum changes, also causes only very minor accumulation of TMCA only. Bile acids make natural and xenobiotic compounds more bioavailable and hence increase absorption from the gut. An alteration of the bile acid pool is likely to lead to altered plasma concentrations of both endogenous metabolites as well as xenobiotics. Furthermore, bile acids themselves interact with nuclear receptors, such as FXR, PXR, CAR, VDR and TGR5, and alteration in the bile acid pool can be expected to have an effect on gene activation [16,21]. This may impact the cytochrome P450 expression and could interfere with drug detoxification mechanisms, finally leading to either a detoxification or toxification of a compound of interest. Furthermore, unconjugated BAs are in general important for controlling the microbial population and the integrity of the intestinal barrier function [16,21]. Regarding the points mentioned above, changes in the bile acid pool might have implications for affecting the intestinal microbiome itself, the gut-liver axis, the immune system and other systems of the body.

Each individual treatment group in this study elicited perturbations in the gut bacterial composition, as observed in the community analysis. Treatments showed a class-specific influence in the bacterial community composition. Clustering analysis of the fecal metabolome showed a virtual identical antibiotic-specific grouping as seen with the 16S microbiome analysis, (see Figure 7a and Supplementary Figure S2), demonstrating that

these two matrixes are highly correlated. Plasma metabolome showed a rather different clustering, indicating that fecal metabolome changes are not well correlated with plasma metabolome changes. Dietary restriction did not induce gut dysbiosis and showed only marginal influences on the fecal metabolome. In contrast, rather explicit effects were seen on the plasma metabolome. Thus, the reduction of dietary nourishment (20% reduced diet) has only very limited effects in the intestinal tract (microbiome and fecal metabolome), whereas the plasma metabolome is profoundly different. Here, we also noted significant gender-specific changes or adaptations. The main purpose behind adding this group of animals fed with a restricted diet was to understand its possible effects on the microbiome and consequently on the metabolome, and it provided rather interesting findings.

Further, cecal and fecal metabolomes are highly comparable; therefore, in rats, fecal profiling should be preferred over cecum, as it is as informative and non-invasive. The strongest correlations obtained were between 16S bacterial families and fecal metabolites, that mainly belong to amino acids, lipids and related metabolite classes.

Key findings from this research work include the following. (1) Administration of different classes of antibiotics showed different compositional effects on the rat fecal microbiome, also showing a class-dependent effect. (2) Streptomycin sulfate and restricted diet showed the most comparable microbiota compared to the rest of the treatments. (3) Compared to plasma metabolome, feces metabolome showed a clear antibiotic-treatment-specific separation, whereas restricted diet separated clearly in the clustering analysis of plasma metabolome, thereby highlighting the fact that dietary restriction changes the host metabolism without significantly altering the gut microbiota. (4) We conclude that the plasma metabolome responds entirely differently to antibiotic treatment compared to both feces and cecum metabolome, for which various correlations with the microbiome could be established. (5) We highlighted several metabolites like Indole derivatives and bile acids as being associated with the presence/absence of specific bacterial families. (6) We associated the accumulation of taurine conjugated bile acids and lack of secondary bile acid formation with antibiotic treatments. The least effective antibiotic was Streptomycin sulfate, which is in line with its antibiotic mode of action. The correlations obtained in this study act as a holistic collection for all the possible bacterial correlations with fecal/plasma metabolites, involving not only already known ones but also some novel or unexplored ones too. Many of these correlations just hint towards a potential relationship, since there are multiple bacterial strains involved in specific biological functions, so it is not just a simple one-to-one correlation, as currently analyzed. Further steps would involve direct network construction using a larger dataset that would explain the correlations in more detail, understanding further the inter-bacterial co-metabolic capacities, which would give a deeper insight into gut microbial metabolism. Understanding the underlying signaling cascades and the gene expression data would give us deeper knowledge about the gut microbiota and host-associated metabolism. An additional step in the future could be to have a use-case with the 16S, metabolome and metagenome data of different samples from animals treated with different substances that are known to perturb the gut microbiota and eventually their associated biological functions. The importance of advancing the field of microbiome-mediated metabolism and the formation of small molecules is not only of academic interest; most of the safety studies with biologically active ingredients and chemicals are done using the rat as the golden standard system. Differences in toxicity outcomes between humans and rats are frequently considered to be related to toxico-dynamic differences, particularly if liver metabolism in both species is assumed to be similar. However, the contribution of the gut microbiome to metabolism, and the potential species differences, have so far been largely ignored. Thus, a database containing the connection between bacterial composition and metabolic capacity for rats would need to be complemented by a similar connectivity for humans. It is of interest to note that despite the profound microbiome and fecal metabolome changes induced by the antibiotics, the effects on the plasma metabolome are rather limited. This, in combination with the mild or absent clinical signs of toxicity, would suggest that at least from a short-term

perspective, even profound microbiome changes do not immediately affect its host's heath. However, such microbiome changes may indeed interfere with the metabolic capacity of its host and could very well change, for instance, the intestinal metabolism of drugs when co-administered in a situation of microbiome dysbiosis. Overall, a combination of 16S bacterial community analysis along with metabolome profiling could allow us to unravel the influence of antibiotics on the gut bacterial composition and metabolism.

Supplementary Materials: The following are available online at https://www.mdpi.com/2036-7481/12/1/8/s1, Figure S1: Shannon Evenness for all the treatments including both sexes and dose groups, Figure S2: Hierarchical clustering (HCA) analysis of 16S gene sequencing data, Figure S3: Relative abundance analysis of bacterial families for individual animals, Figure S4: Principle Component Analysis (PCA) of feces metabolites from different treatments, Figure S5: Dendrogram showing hierarchical clustering of cecum metabolites of different treatments, dose groups and sex, Figure S6: Principle Component Analysis (PCA) of cecum metabolites from different treatments, Figure S7: Principle Component Analysis (PCA) of plasma metabolites from different treatments, Figure S8: Boxplots comparing between different metabolome matrices, Figure S9: Shannon true diversity analysis of six antibiotic treatments focused for both male and female Wistar rats; Table S1: Relative changes in body weight and food consumption of male and female rats, Tables S2–S8: Top 25 (both directions) of plasma altered metabolites ($p < 0.1$) for both females and males respectively for restricted diet, Streptomycin sulfate, Roxithromycin, Sparfloxacin, Vancomycin, Clindamycin and Lincomycin hydrochloride respectively, Tables S9–S15: Feces altered metabolites ($p < 0.1$) for both females (left) and males (right) respectively for restricted diet, Streptomycin sulfate, Roxithromycin, Sparfloxacin, Vancomycin, Clindamycin and Lincomycin hydrochloride respectively, Table S16: The table below shows DESeq2 analysis results from the low dose (LD) groups of all the treatments, Table S17: Fold changes of different bile acid levels in the feces and plasma matrices of male and female Wistar rats of Lincomycin hydrochloride treatment.

References

1. Li, D.; Chen, H.; Mao, B.; Yang, Q.; Zhao, J.; Gu, Z.; Zhang, H.; Chen, Y.Q.; Chen, W. Microbial Biogeography and Core Microbiota of the Rat Digestive Tract. *Sci. Rep.* **2017**, *7*, 45840. [CrossRef]
2. Gill, S.R.; Pop, M.; DeBoy, R.T.; Eckburg, P.B.; Turnbaugh, P.J.; Samuel, B.S.; Gordon, J.I.; Relman, D.A.; Fraser-Liggett, C.M.; Nelson, K.E. Metagenomic Analysis of the Human Distal Gut Microbiome. *Science* **2006**, *312*, 1355–1359. [CrossRef] [PubMed]
3. Sender, R.; Fuchs, S.; Milo, R. Revised Estimates for the Number of Human and Bacteria Cells in the Body. *PLoS Biol.* **2016**, *14*, e1002533. [CrossRef]
4. Zimmermann, M.; Zimmermann-Kogadeeva, M.; Wegmann, R.; Goodman, A.L. Mapping human microbiome drug metabolism by gut bacteria and their genes. *Nat. Cell Biol.* **2019**, *570*, 462–467. [CrossRef]
5. Clarke, G.; Sandhu, K.V.; Griffin, B.T.; Dinan, T.G.; Cryan, J.F.; Hyland, N.P. Gut Reactions: Breaking Down Xenobiotic–Microbiome Interactions. *Pharmacol. Rev.* **2019**, *71*, 198–224. [CrossRef]
6. ECETOC. *Microbiome Expert Workshop Report (Porto, 8–9 July 2019)*; 2078-7219-036; ECETOC: Brussels, Belgium, 2020.
7. Bourassa, M.W.; Alim, I.; Bultman, S.J.; Ratan, R.R. Butyrate, neuroepigenetics and the gut microbiome: Can a high fiber diet improve brain health? *Neurosci. Lett.* **2016**, *625*, 56–63. [CrossRef]
8. Maier, L.; Pruteanu, M.; Kuhn, M.; Zeller, G.; Telzerow, A.; Anderson, E.E.; Brochado, A.R.; Fernandez, K.C.; Dose, H.; Mori, H.; et al. Extensive impact of non-antibiotic drugs on human gut bacteria. *Nat. Cell Biol.* **2018**, *555*, 623–628. [CrossRef] [PubMed]
9. Nicholson, J.K.; Holmes, E.; Kinross, J.; Burcelin, R.; Gibson, G.; Jia, W.; Pettersson, S. Host-Gut Microbiota Metabolic Interactions. *Science* **2012**, *336*, 1262–1267. [CrossRef] [PubMed]
10. Zheng, H.; Chen, M.; Li, Y.; Wang, Y.; Wei, L.; Liao, Z.; Wang, M.; Ma, F.; Liao, Q.; Xie, Z. Modulation of Gut Microbiome Composition and Function in Experimental Colitis Treated with Sulfasalazine. *Front. Microbiol.* **2017**, *8*, 1703. [CrossRef] [PubMed]
11. Ghaisas, S.; Maher, J.; Kanthasamy, A. Gut microbiome in health and disease: Linking the microbiome–gut–brain axis and environmental factors in the pathogenesis of systemic and neurodegenerative diseases. *Pharmacol. Ther.* **2016**, *158*, 52–62. [CrossRef]
12. Ridaura, V.K.; Faith, J.J.; Rey, F.E.; Cheng, J.; Duncan, A.E.; Kau, A.L.; Griffin, N.W.; Lombard, V.; Henrissat, B.; Bain, J.R.; et al. Gut Microbiota from Twins Discordant for Obesity Modulate Metabolism in Mice. *Science* **2013**, *341*, 1241214. [CrossRef]
13. Anders, M. Metabolism of drugs by the kidney. *Kidney Int.* **1980**, *18*, 636–647. [CrossRef]
14. Behr, C.; Kamp, H.; Fabian, E.; Krennrich, G.; Mellert, W.; Peter, E.; Strauss, V.; Walk, T.; Rietjens, I.M.C.M.; Van Ravenzwaay, B. Gut microbiome-related metabolic changes in plasma of antibiotic-treated rats. *Arch. Toxicol.* **2017**, *91*, 3439–3454. [CrossRef]
15. Behr, C.; Ramírez-Hincapié, S.; Cameron, H.; Strauss, V.; Walk, T.; Herold, M.; Beekmann, K.; Rietjens, I.; Van Ravenzwaay, B. Impact of lincosamides antibiotics on the composition of the rat gut microbiota and the metabolite profile of plasma and feces. *Toxicol. Lett.* **2018**, *296*, 139–151. [CrossRef] [PubMed]
16. Behr, C.; Slopianka, M.; Haake, V.; Strauss, V.; Sperber, S.; Kamp, H.; Walk, T.; Beekmann, K.; Rietjens, I.; Van Ravenzwaay, B. Analysis of metabolome changes in the bile acid pool in feces and plasma of antibiotic-treated rats. *Toxicol. Appl. Pharmacol.* **2019**, *363*, 79–87. [CrossRef] [PubMed]
17. Behr, C.; Sperber, S.; Jiang, X.; Strauss, V.; Kamp, H.; Walk, T.; Herold, M.; Beekmann, K.; Rietjens, I.; van Ravenzwaay, B. Microbiome-related metabolite changes in gut tissue, cecum content and feces of rats treated with antibiotics. *Toxicol. Appl. Pharmacol.* **2018**, *355*, 198–210. [CrossRef]
18. Van Ravenzwaay, B.; Herold, M.; Kamp, H.; Kapp, M.; Fabian, E.; Looser, R.; Krennrich, G.; Mellert, W.; Prokoudine, A.; Strauss, V.; et al. Metabolomics: A tool for early detection of toxicological effects and an opportunity for biology based grouping of chemicals—From QSAR to QBAR. *Mutat. Res. Toxicol. Environ. Mutagen.* **2012**, *746*, 144–150. [CrossRef]
19. Van Ravenzwaay, B.; Sperber, S.; Lemke, O.; Fabian, E.; Faulhammer, F.; Kamp, H.; Mellert, W.; Strauss, V.; Strigun, A.; Peter, E.; et al. Metabolomics as read-across tool: A case study with phenoxy herbicides. *Regul. Toxicol. Pharmacol.* **2016**, *81*, 288–304. [CrossRef]
20. Van Ravenzwaay, B.; Cunha, G.C.-P.; Leibold, E.; Looser, R.; Mellert, W.; Prokoudine, A.; Walk, T.; Wiemer, J. The use of metabolomics for the discovery of new biomarkers of effect. *Toxicol. Lett.* **2007**, *172*, 21–28. [CrossRef]
21. De Bruijn, V.; Behr, C.; Sperber, S.; Walk, T.; Ternes, P.; Slopianka, M.; Haake, V.; Beekmann, K.; Van Ravenzwaay, B. Antibiotic-Induced Changes in Microbiome-Related Metabolites and Bile Acids in Rat Plasma. *Metabolites* **2020**, *10*, 242. [CrossRef]
22. R Core Team. *R: A Language and Environment for Statistical Computing*; R Core Team: Vienna, Austria, 2020.
23. RStudio Team. *RStudio: Integrated Development Environment for R*; RStudio: Boston, MA, USA, 2020.
24. Troyanskaya, O.G.; Cantor, M.; Sherlock, G.; Brown, P.O.; Hastie, T.; Tibshirani, R.; Botstein, D.; Altman, R.B. Missing value estimation methods for DNA microarrays. *Bioinformatics* **2001**, *17*, 520–525. [CrossRef]
25. Callahan, B.J.; Mcmurdie, P.J.; Rosen, M.J.; Han, A.W.; Johnson, A.J.A.; Holmes, S.P. DADA2: High-resolution sample inference from Illumina amplicon data. *Nat. Methods* **2016**, *13*, 581–583. [CrossRef] [PubMed]
26. Martin, M. Cutadapt removes adapter sequences from high-throughput sequencing reads. *EMBnet J.* **2011**, *17*, 10–12. [CrossRef]
27. Cole, J.R.; Wang, Q.; Fish, J.A.; Chai, B.; McGarrell, D.M.; Sun, Y.; Brown, C.T.; Porras-Alfaro, A.; Kuske, C.R.; Tiedje, J.M. Ribosomal Database Project: Data and tools for high throughput rRNA analysis. *Nucleic Acids Res.* **2014**, *42*, D633–D642. [CrossRef] [PubMed]
28. Love, M.I.; Huber, W.; Anders, S. Moderated estimation of fold change and dispersion for RNA-seq data with DESeq2. *Genome Biol.* **2014**, *15*, 550. [CrossRef]

29. McMurdie, P.J.; Holmes, S. PHYLOSEQ: A Bioconductor Package for Handling and Analysis of High-Throughput Phylogenetic Sequence Data. In *Biocomputing*; Springer: Berlin/Heidelberg, Germany, 2012; pp. 235–246. [CrossRef]

30. Paulson, J.N.; Stine, O.C.; Bravo, H.C.; Pop, M. Differential abundance analysis for microbial marker-gene surveys. *Nat. Methods* **2013**, *10*, 1200–1202. [CrossRef]

31. Oksanen, J.; Blanchet, F.G.; Kindt, R.; Legendre, P.; Minchin, P.R.; O'Hara, R. *Package 'Vegan'. Community Ecology Package, Version 2*; R Core Team: Vienna, Austria, 2013.

32. Liu, C.M.; Bs, K.S.; Nordstrom, L.; Dwan, M.G.; Moss, O.L.; Contente-Cuomo, T.L.; Keim, P.; Price, L.B.; Lane, A.P.; Bs, M.G.D.; et al. Medical therapy reduces microbiota diversity and evenness in surgically recalcitrant chronic rhinosinusitis. *Int. Forum Allergy Rhinol.* **2013**, *3*, 775–781. [CrossRef] [PubMed]

33. Fraumene, C.; Manghina, V.; Cadoni, E.; Marongiu, F.; Abbondio, M.; Serra, M.; Palomba, A.; Tanca, A.; Laconi, E.; Uzzau, S. Caloric restriction promotes rapid expansion and long-lasting increase of Lactobacillus in the rat fecal microbiota. *Gut Microbes* **2017**, *9*, 104–114. [CrossRef]

34. Verdier, L.; Bertho, G.; Gharbi-Benarous, J.; Girault, J.-P. Lincomycin and clindamycin conformations. A fragment shared by macrolides, ketolides and lincosamides determined from TRNOE ribosome-bound conformations. *Bioorganic Med. Chem.* **2000**, *8*, 1225–1243. [CrossRef]

35. Zhou, G.; An, Z.; Zhao, W.; Hong, Y.; Xin, H.; Ning, X.; Wang, J. Sex differences in outcomes after stroke among patients with low total cholesterol levels: A large hospital-based prospective study. *Biol. Sex Differ.* **2016**, *7*, 62. [CrossRef]

36. Kim, Y.S.; Unno, T.; Kim, B.-Y.; Park, M.-S. Sex Differences in Gut Microbiota. *World J. Men's Health* **2020**, *38*, 48–60. [CrossRef]

37. Wishart, D.S. DrugBank: A comprehensive resource for in silico drug discovery and exploration. *Nucleic Acids Res.* **2006**, *34*, D668–D672. [CrossRef]

38. Bao, H.-D.; Pang, M.-D.; Olaniran, A.; Zhang, X.-H.; Zhang, H.; Zhou, Y.; Sun, L.-C.; Schmidt, S.; Wang, R. Alterations in the diversity and composition of mice gut microbiota by lytic or temperate gut phage treatment. *Appl. Microbiol. Biotechnol.* **2018**, *102*, 10219–10230. [CrossRef]

39. Zhang, C.; Li, X.; Liu, L.; Gao, L.; Ou, S.; Luo, J.; Peng, X. Roxithromycin regulates intestinal microbiota and alters colonic epithelial gene expression. *Appl. Microbiol. Biotechnol.* **2018**, *102*, 9303–9316. [CrossRef] [PubMed]

40. Zheng, X.; Wang, S.; Jia, W. Calorie restriction and its impact on gut microbial composition and global metabolism. *Front. Med.* **2018**, *12*, 634–644. [CrossRef]

41. Zeng, H.; Grapov, D.; Jackson, M.I.; Fahrmann, J.F.; Fiehn, O.; Combs, G.F. Integrating Multiple Analytical Datasets to Compare Metabolite Profiles of Mouse Colonic-Cecal Contents and Feces. *Metabolites* **2015**, *5*, 489–501. [CrossRef] [PubMed]

42. Ninnes, C.E.; Waas, J.R.; Ling, N.; Nakagawa, S.; Banks, J.C.; Bell, D.G.; Bright, A.; Carey, P.W.; Chandler, J.; Hudson, Q.J.; et al. Comparing plasma and faecal measures of steroid hormones in Adelie penguins Pygoscelis adeliae. *J. Comp. Physiol. B* **2009**, *180*, 83–94. [CrossRef] [PubMed]

43. Fujisaka, S.; Avila-Pacheco, J.; Soto, M.; Kostic, A.; Dreyfuss, J.M.; Pan, H.; Ussar, S.; Altindis, E.; Li, N.; Bry, L.; et al. Diet, Genetics, and the Gut Microbiome Drive Dynamic Changes in Plasma Metabolites. *Cell Rep.* **2018**, *22*, 3072–3086. [CrossRef] [PubMed]

44. Goldstein, E.J.; Citron, D.M.; Gerardo, S.H.; Hudspeth, M.; Merriam, C.V. Comparative in vitro activities of DU-6859a, levofloxacin, ofloxacin, sparfloxacin, and ciprofloxacin against 387 aerobic and anaerobic bite wound isolates. *Antimicrob. Agents Chemother.* **1997**, *41*, 1193–1195. [CrossRef] [PubMed]

45. Bahar, H.; Torun, M.M.; Demirci, M.; Kocazeybek, B. Antimicrobial Resistance and β-Lactamase Production of Clinical Isolates of Prevotella and Porphyromonas Species. *Chemotherapy* **2005**, *51*, 9–14. [CrossRef]

46. Dai, Z.-L. Amino acid metabolism in intestinal bacteria: Links between gut ecology and host health. *Front. Biosci.* **2011**, *16*, 1768–1786. [CrossRef]

47. Alkhalaf, L.M.; Ryan, K.S. Biosynthetic Manipulation of Tryptophan in Bacteria: Pathways and Mechanisms. *Chem. Biol.* **2015**, *22*, 317–328. [CrossRef]

48. Rikitake, K.; Oka, I.; Ando, M.; Yoshimoto, T.; Tsuru, D. Creatinine Amidohydrolase (Creatininase) from Pseudomonas putida: ePurification and Some Properties1. *J. Biochem.* **1979**, *86*, 1109–1117. [CrossRef]

49. Idris, E.E.; Iglesias, D.J.; Talon, M.; Borriss, R. Tryptophan-Dependent Production of Indole-3-Acetic Acid (IAA) Affects Level of Plant Growth Promotion by Bacillus amyloliquefaciens FZB42. *Mol. Plant-Microbe Interact.* **2007**, *20*, 619–626. [CrossRef]

50. Sanguinetti, E.; Collado, M.C.; Marrachelli, V.G.; Monleon, D.; Selma-Royo, M.; Pardo-Tendero, M.M.; Burchielli, S.; Iozzo, P. Microbiome-metabolome signatures in mice genetically prone to develop dementia, fed a normal or fatty diet. *Sci. Rep.* **2018**, *8*, 1–13. [CrossRef]

51. Apper, E.; Privet, L.; Taminiau, B.; Le Bourgot, C.; Svilar, L.; Martin, J.-C.; Diez, M. Relationships between Gut Microbiota, Metabolome, Body Weight, and Glucose Homeostasis of Obese Dogs Fed with Diets Differing in Prebiotic and Protein Content. *Microorganisms* **2020**, *8*, 513. [CrossRef]

52. Steinway, S.N.; Biggs, M.B.; Jr, T.P.L.; Papin, J.A.; Albert, R. Inference of Network Dynamics and Metabolic Interactions in the Gut Microbiome. *PLoS Comput. Biol.* **2015**, *11*, e1004338. [CrossRef]

53. Zhao, Z.-H.; Xin, F.-Z.; Xue, Y.; Hu, Z.; Han, Y.; Ma, F.; Zhou, D.; Liu, X.-L.; Cui, A.; Liu, Z.; et al. Indole-3-propionic acid inhibits gut dysbiosis and endotoxin leakage to attenuate steatohepatitis in rats. *Exp. Mol. Med.* **2019**, *51*, 1–14. [CrossRef]

54. Louis, P.; Flint, H.J. Formation of propionate and butyrate by the human colonic microbiota. *Environ. Microbiol.* **2017**, *19*, 29–41. [CrossRef] [PubMed]

55. Jazani, N.H.; Savoj, J.; Lustgarten, M.; Lau, W.L.; Vaziri, N.D. Impact of Gut Dysbiosis on Neurohormonal Pathways in Chronic Kidney Disease. *Diseases* **2019**, *7*, 21. [CrossRef] [PubMed]

56. Zheng, X.; Xie, G.; Zhao, A.; Zhao, L.; Yao, C.; Chiu, N.H.L.; Zhou, Z.; Bao, Y.; Jia, W.; Nicholson, J.K.; et al. The Footprints of Gut Microbial–Mammalian Co-Metabolism. *J. Proteome Res.* **2011**, *10*, 5512–5522. [CrossRef] [PubMed]

57. Wahlström, A.; Sayin, S.I.; Marschall, H.-U.; Bäckhed, F. Intestinal Crosstalk between Bile Acids and Microbiota and Its Impact on Host Metabolism. *Cell Metab.* **2016**, *24*, 41–50. [CrossRef]

58. Martin, F.J.; Dumas, M.; Wang, Y.; Legido-Quigley, C.; Yap, I.K.S.; Tang, H.; Zirah, S.; Murphy, G.M.; Cloarec, O.; Lindon, J.C.; et al. A top-down systems biology view of microbiome-mammalian metabolic interactions in a mouse model. *Mol. Syst. Biol.* **2007**, *3*, 112. [CrossRef] [PubMed]

59. Di Ciaula, A.; Garruti, G.; Baccetto, R.L.; Molina-Molina, E.; Bonfrate, L.; Wang, D.Q.-H.; Portincasa, P. Bile Acid Physiology. *Ann. Hepatol.* **2017**, *16*, S4–S14. [CrossRef] [PubMed]

60. Li, J.; Dawson, P.A. Animal models to study bile acid metabolism. *Biochim. Biophys. Acta (BBA)-Mol. Basis Dis.* **2019**, *1865*, 895–911. [CrossRef] [PubMed]